

THE DESIGN OF STEEL STRUCTURES
A SECOND-ORDER APPROACH

By

Darryl Douglas Matson

B. A. Sc. (Civil Engineering) University of British Columbia

A THESIS SUBMITTED IN PARTIAL FULFILLMENT OF
THE REQUIREMENTS FOR THE DEGREE OF
MASTERS OF APPLIED SCIENCE

in

THE FACULTY OF GRADUATE STUDIES
CIVIL ENGINEERING

We accept this thesis as conforming
to the required standard

THE UNIVERSITY OF BRITISH COLUMBIA

Darryl Douglas Matson

© Darryl Douglas Matson, 1989

In presenting this thesis in partial fulfilment of the requirements for an advanced degree at the University of British Columbia, I agree that the Library shall make it freely available for reference and study. I further agree that permission for extensive copying of this thesis for scholarly purposes may be granted by the head of my department or by his or her representatives. It is understood that copying or publication of this thesis for financial gain shall not be allowed without my written permission.

Department of CIVIL ENGINEERING

The University of British Columbia
Vancouver, Canada

Date OCTOBER 13, 1989

Abstract

The wide spread use of limit states design procedures in both the Canadian and American steel design codes has created a need for a better understanding of how structures behave. Current design practice, however, allows and often encourages engineers to use an approximate linear analysis to determine the member forces in a structure. This is then followed by an even more approximate amplification of forces through the use of several design equations. It is believed that this practice is no longer acceptable as more accurate second-order computer programs have become a very practical alternative.

With this as motivation, this thesis will provide a comparison between a second-order computer program available at the University of British Columbia called ULA (Ultimate Load Analysis) and the Canadian and American building code designs, CAN3-S16.1-M84 and LRFD 1986 respectively.

It was felt that ULA should be verified, even though the theory it is based on is well established. Thus, ULA was used to generate a load versus L/r curve for a pin ended column (with the parameters modified slightly to allow direct comparison with the curves available in the codes). ULA was then used to predict load-deflection curves for two existing test frames. The resulting curves compared well with the test data.

To ensure simplicity, the building codes make several approximations in the derivation of their design equations. This results in the equations being applicable to a very narrow range of structures. Specifically, the equations apply to rigidly connected frames in which all of the columns reach their critical buckling load simultaneously. Consequently, the results from ULA were compared to the codes for structures of this type. It was found that the codes were conservative for these structures in relation to the results from ULA,

yet the amount of conservatism varied greatly between structures. That is, the codes are not consistent in how conservative they are. Results from ULA were then compared to the codes for structures that do not satisfy all of the code limitations. Although using the codes to design structures beyond the limit of applicability is not a recommended practice, engineers do use the codes to design all types of structures, with little appreciation for the applicability limits. Consequently, it was deemed appropriate to extend this study to such structures. Though only a few were investigated, it was found that the codes were unreliable, being highly conservative, very accurate, or in one case highly unconservative when compared to the results from ULA.

Table of Contents

Abstract	ii
List of Tables	vii
List of Figures	viii
Acknowledgements	x
1 Introduction	1
1.1 Basic Design Philosophies	1
1.2 Reserve Capacity	2
1.3 The 1984 Canadian Steel Code	3
1.3.1 Introduction	3
1.3.2 Strength Equations	5
1.3.3 Stability Equation	8
1.3.4 Column Effective Length	10
1.3.5 Limit of Application	16
1.4 The 1986 American Steel Code	17
2 An Alternative Design Method	22
2.1 General	22
2.2 ULA Theory and Underlying Assumptions	23
2.2.1 Second-Order Elasto-Plastic Analysis with Moment-Axial Interaction	24
2.2.2 Moment Curvature	30

3	Verification of ULA	33
3.1	General	33
3.2	A Centrally Loaded, Initially Eccentric Column	33
3.2.1	Governing Parameters	33
3.2.2	Variation of Parameters	35
3.3	Yaramci Test Frame B	38
3.4	Baker Pin-Based Test Frame	39
4	Structures Within The Code Limits	43
4.1	Introduction	43
4.2	Group One : Fix-Based Portal Frames	43
4.2.1	General	43
4.2.2	Canadian Code Design, Fix-Based Frames	44
4.2.3	American Code Design, Fix-Based Frames	45
4.3	Group Two : Pin-Based Portal Frames	47
4.3.1	General	47
4.3.2	Canadian Code Design, Pin-Based Frames	47
4.3.3	American Code Design, Pin-Based Frames	49
4.4	Group Three : Laterally Supported Fix-Based Portal Frames	49
4.4.1	General	49
4.4.2	Canadian Code Design, Laterally Supported Fix-Based Frames . .	51
4.4.3	American Code Design, Laterally Supported Fix-Based Frames . .	51
4.5	Group Four : Laterally Supported Pin-Based Portal Frames	52
4.5.1	General	52
4.5.2	Canadian Code Design, Laterally Supported Pin-Based Frames . .	53
4.5.3	American Code Design, Laterally Supported Pin-Based Frames . .	54

5	Structures Beyond the Code Limits	56
5.1	Introduction	56
5.2	Example Number One : Pin-Ended A-Frame	56
5.2.1	General	56
5.2.2	Effective Length Factor, k	57
5.2.3	Code Design of Member CE	59
5.3	Example Number Two : Single Fix-Based, Pin-Ended Frame	65
5.3.1	General	65
5.3.2	Code Design	66
5.4	Example Number Three : Five Storey Frame, Tension on One Side	68
5.4.1	General	68
5.4.2	Code Design	69
5.5	Example Number Four : Four Storey Frame, Multiple Column Lengths	69
5.5.1	General	69
5.6	Example Number Five : Tied and Fixed Arch	71
5.6.1	General	71
5.7	Example Number Six : Overpass	73
5.7.1	General	73
6	Conclusions And Recomendations	75
6.1	Conclusions	75
6.2	Recommendations	76
6.3	Further Research	77
	Bibliography	78

List of Tables

3.1	Measured Values For Yaramci Test Frame B	39
4.2	$\frac{HL}{0.9Z\sigma_y}$ Values For Fix-Based Frames	46
4.3	$\frac{HL}{0.9Z\sigma_y}$ Values For Pin-Based Frames	49
4.4	$\frac{wL^2}{0.9Z\sigma_y}$ Values For Laterally Supported Fix-Based Frames	52
4.5	$\frac{wL^2}{0.9Z\sigma_y}$ Values For Laterally Supported Pin-Based Frames	55
5.6	$\frac{P}{0.9A\sigma_y}$ Results For A-Frame : Vertical Load	62
5.7	$\frac{P}{0.9A\sigma_y}$ Results For A-Frame : Horizontal Load	64
5.8	$\frac{0.02PL}{0.9Z\sigma_y}$ Values For Single Fix-Based, Pin-Ended Frame	67
5.9	$\frac{3P}{0.9A\sigma_y}$ Results For Five Storey Frame	69
5.10	$\frac{P}{0.9A\sigma_y}$ Results For Four Storey Frame	71

List of Figures

1.1	Full Plastification of an I-Shaped Section	5
1.2	Values of M_{pc} for W-shapes	6
1.3	Canadian Moment-Axial Failure Surface	7
1.4	Simple Beam-Column with Equal End Moments	8
1.5	Schematic Representation of M_{eq}	9
1.6	Theoretical and Approximate Equivalent Moment Factor, ω	11
1.7	Sway-Prevented Column	13
1.8	Sway-Permitted Column	15
1.9	American Moment-Axial Failure Surface	19
2.10	Moment-Axial Failure Surface Used in ULA	26
2.11	Joint Before and After Hinge Placement	27
2.12	Hinge Formation Sequence	28
2.13	Second-Order Elasto-Plastic Response	29
2.14	Idealized Elasto-Plastic Behaviour	30
2.15	Moment-Axial-Curvature Relationship	31
2.16	Cooling Residual Stress Pattern	31
2.17	Effect of Elasto-Plastic Assumption	32
3.18	Pin Ended Column Used in the Computer Analysis	34
3.19	Variation of y/r for a Simple Column	36
3.20	Variation of ϵ_y for a Simple Column	37
3.21	Load-Deflection Curves for Yaramci Test Frame B	40

3.22	Load-Deflection Curves for Baker Test Frame	41
4.23	Fix-Based Portal Frame	44
4.24	Pin-Based Portal Frame	48
4.25	Laterally Supported Fix-Based Portal Frame	50
4.26	Laterally Supported Pin-Based Portal Frame	53
5.27	Pin-Ended A-Frame	58
5.28	Variation of k Against θ for Member CE	59
5.29	A-Frame Computer Model : Vertical Load	61
5.30	A-Frame Computer Model : Horizontal Load	63
5.31	Single Fix-Based, Pin-Ended Frame	65
5.32	Five Storey Frame: Tension on One Side	68
5.33	Four Storey Frame: Multiple Column Lengths	70
5.34	Fixed And Tied Arch	72
5.35	Overpass	74

Acknowledgements

I would like to express my sincere appreciation to Dr. Roy F. Hooley for his support and advise through the course of this work.

Chapter 1

Introduction

1.1 Basic Design Philosophies

Basic structural design philosophies have evolved over the years to more realistically predict possible field conditions. Allowable, or working stress design was used for many years, and is still widely used today. In allowable stress design, the combined stress due to dead and live loads is less than some allowable stress. This allowable stress is usually the yield stress of the material divided by a factor of safety, N . i.e.:

$$\sigma_{DL} + \sigma_{LL} \leq \frac{\sigma_y}{N} \quad (1.1)$$

where:

σ_{DL} = Stress due to applied Dead Loads

σ_{LL} = Stress due to applied Live Loads

σ_y = Material yield stress

N = Factor of safety

Equation 1.1 implies that both the dead and live loads have the same factor of safety. More recent statistical studies, however, have shown that the variation in the live load is much greater than that of the dead load. Therefore, the factor of safety for live loads should be greater than that for dead loads. These studies lead to what is termed a probability based, limit states design. The objective of this design method is to ensure that the probability of reaching a given limit state, such as the formation of a plastic

hinge, is below an acceptable limit. The resulting design philosophy is as follows:

$$N_1 D_{DL} + N_2 D_{LL} \leq \phi R \quad (1.2)$$

where:

$N_1 D_{DL}$ = Maximum probable demand due to applied dead loads

$N_2 D_{LL}$ = Maximum probable demand due to applied live loads

R = Resistance of a member, connection, or structure, to the applied loads

ϕ = Capacity reduction factor accounting for material variation, fabrication errors, etc.

A slight change in nomenclature accompanies the new design method such that N_1 and N_2 are referred to as load factors, rather than safety factors as they are found on the left hand side of Eq. 1.2.

This thesis is concerned with the current limit states design of steel structures, in particular, Class 1 and 2, laterally supported I-shaped steel beam-columns. Thus the design procedure for beam-columns employed by the 1984 Canadian [1] and 1986 American [2] steel codes will be reviewed. The codes will then be compared to a more precise second-order computer program.

1.2 Reserve Capacity

Current design practices, both Canadian and American, employ the formation of the first plastic hinge as one of their limit states design criteria. That is, when the first hinge forms in the structure, the structure is considered to have failed.

Very slender and statically determinant structures do in fact fail at or before the formation of the first hinge. However, stiffer indeterminant structures are capable of carrying additional load above that required to form the first hinge. Clearly, the maximum

load a structure is capable of carrying is that required to cause collapse. The difference between the collapse load and the load required to form the first hinge is referred to as the structure's reserve capacity. Because of their choice of limit states, both codes ignore this reserve.

1.3 The 1984 Canadian Steel Code

1.3.1 Introduction

The Canadian steel code, CAN3-S16.1-M84, allows an engineer to design Class 1 and 2, I-shaped beam-columns in one of two ways. These are:

a) the use of a second-order analysis to determine the member forces, combined with the "side-sway prevented" nomograph for approximating the member's effective length, or

b) the use of a linear analysis to determine the member forces, combined with the "side-sway permitted" nomograph for approximating the effective length.

Once the designer has made a decision as to which of the above methods he will use, the code requires that he check three interaction equations. Namely, for uniaxial bending, fully supported laterally:

$$\frac{M_f}{\phi Z \sigma_y} \leq 1.0 \quad (1.3)$$

$$\frac{C_f}{\phi A \sigma_y} + \frac{0.85 M_f}{\phi Z \sigma_y} \leq 1.0 \quad (1.4)$$

$$\frac{C_f}{C_r} + \frac{\omega M_f}{\phi Z \sigma_y \left(1 - \frac{C_f}{C_c}\right)} \leq 1.0 \quad (1.5)$$

where:

M_f = Largest member end moment caused by the factored loads, or in the case of simply supported members, the maximum moment in the member

C_f = Axial load caused by factored loads

ϕ = Material reduction factor, $\phi = 0.90$ for structural steel

Z = Plastic section modulus of the member

A = Cross section area of the member

σ_y = Material yield stress

C_e = Euler load = $\frac{\pi^2 EI}{(kL)^2}$

k = Effective length of column determined from nomograph, see Sec. 1.3.4 below

E = Young's modulus

C_r = Column resistance with zero moment = $f\left(\frac{kL}{r}\right)$, see eq. 1.6 below

r = Radius of gyration

ω = Equivalent moment factor, see Sec. 1.3.3 below

Equations 1.3 and 1.4 are classified as strength checks, and have a theoretical base.

Equation 1.5 is classified as a stability check, and is empirical in nature.

The expression given in the code for C_r is a rather complex function and is as follows:

$$\begin{aligned}
 C_r &= \phi C_y & 0 \leq \lambda \leq 0.15 \\
 C_r &= \phi C_y (1.035 - 0.202\lambda - 0.222\lambda^2) & 0.15 < \lambda \leq 1.0 \\
 C_r &= \phi C_y (-0.111 + 0.636\lambda^{-1} + 0.087\lambda^{-2}) & 1.0 < \lambda \leq 2.0 \\
 C_r &= \phi C_y (0.009 + 0.877\lambda^{-2}) & 2.0 < \lambda \leq 3.6 \\
 C_r &= \phi C_y \lambda^{-2} & 3.6 < \lambda
 \end{aligned} \tag{1.6}$$

where

$$\lambda = \frac{kL}{r} \sqrt{\frac{\sigma_y}{\pi^2 E}} \tag{1.7}$$

and C_y = Maximum axial capacity = $A\sigma_y$.

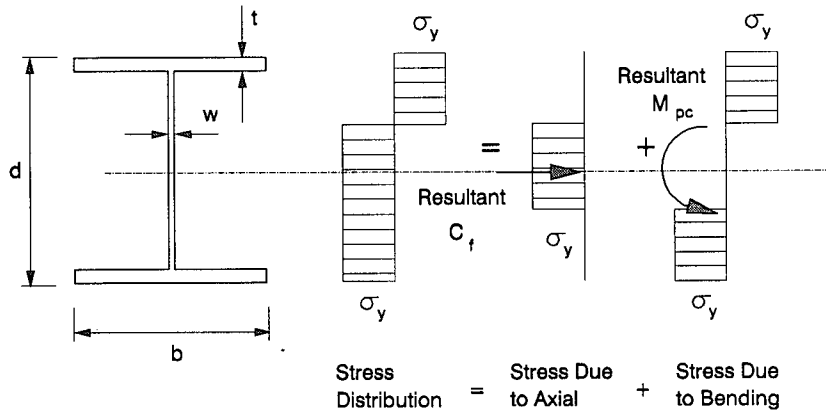


Figure 1.1: Full Plastification of an I-Shaped Section

1.3.2 Strength Equations

Equations 1.3 and 1.4 attempt to ensure that the moment at the end of the beam-column is not greater than the member is capable of developing under the action of the axial load, C_f . These equations are a linear approximation of the moment capacity, based on full plastification of the I-shaped cross section as shown in Fig. 1.1.

Using the nomenclature in Fig. 1.1, the value of M_{pc} , the reduced moment capacity, is given in non-dimensional form by the following:

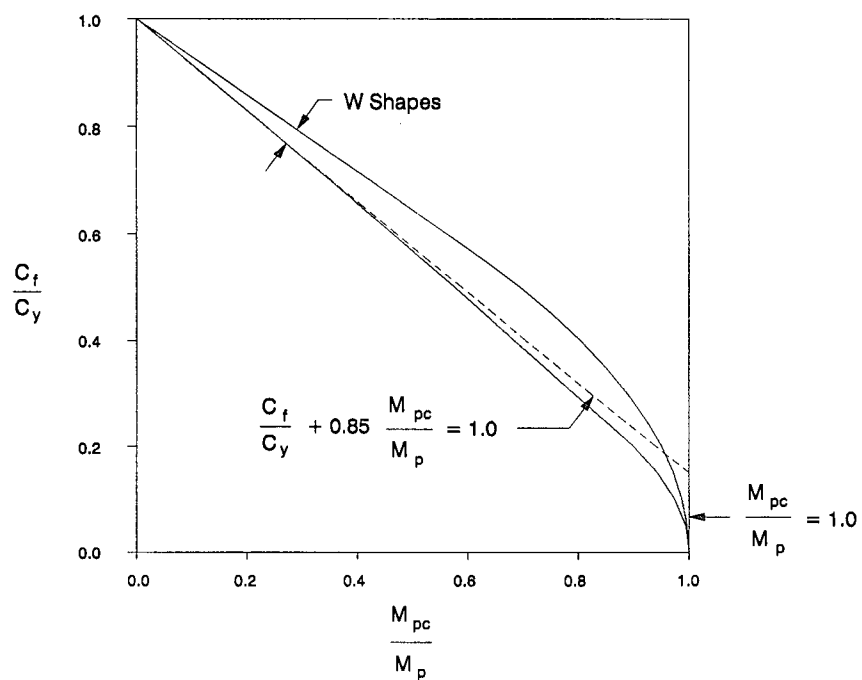
$$\frac{M_{pc}}{M_p} = 1 - \frac{A^2}{4wZ} \left(\frac{C_f}{C_y} \right)^2 \quad 0 \leq \frac{C_f}{C_y} \leq \frac{w(d-2t)}{A} \quad (1.8)$$

$$\frac{M_{pc}}{M_p} = \frac{A}{2Z} \left\{ d \left(1 - \frac{C_f}{C_y} \right) - \frac{A}{2b} \left(1 - \frac{C_f}{C_y} \right)^2 \right\} \quad \frac{w(d-2t)}{A} < \frac{C_f}{C_y} \leq 1.0 \quad (1.9)$$

where:

$$M_p = Z\sigma_y = \text{Plastic moment of section}$$

These two equations have been plotted for various W-shaped sections in Fig. 1.2.

Figure 1.2: Values of M_{pc} for W-shapes

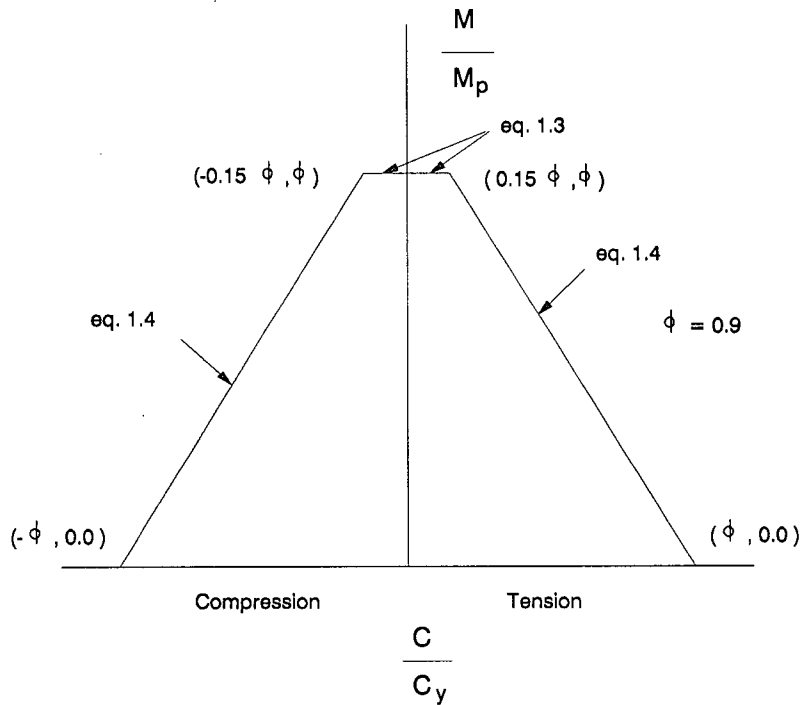


Figure 1.3: Canadian Moment-Axial Failure Surface

It is obvious that a combination of Equations 1.3 and 1.4 with $\phi = 1.0$ gives a very good approximation to the theory. It must be noted, though, that Equations 1.3 and 1.4 take no account of stability effects. Thus, if the designer calculates the second-order moments in his analysis, i.e. the analysis procedure includes stability effects, then Equations 1.3 and 1.4 apply for members of all lengths. If, however, he calculates only linear moments, i.e. no stability effects included, equations 1.3 and 1.4 only apply to members of zero length [3].

Extending plastification to tension as well as compression, a yield or failure surface can be developed for a given structural shape. The surface used by the Canadian code for I-shapes is illustrated in Fig. 1.3.



Figure 1.4: Simple Beam-Column with Equal End Moments

1.3.3 Stability Equation

Equation 1.5 of Section 1.3.1 is termed the stability equation by the Canadian code and is empirical in nature. It has been modified since its inception, when it was simply (in limit states format)

$$\frac{C_f}{C_r} + \frac{M_f}{M_r} \leq 1.0 \quad (1.10)$$

where:

M_f = Member end moment

C_f = Member axial load

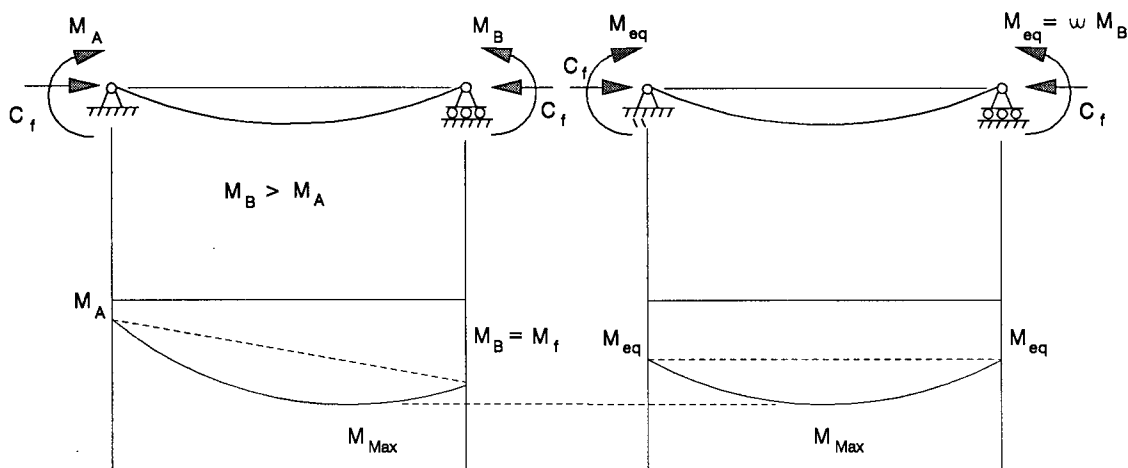
$M_r = S\sigma_y$ = Collapse moment for simple bending

C_r = Critical axial load for concentric buckling = $f \left(\frac{kL}{r} \right)$

This equation was based on research done on pin-ended beam-columns with applied equal and opposite end moments [5] as shown in Fig. 1.4.

Early researchers suggested the inclusion of the now familiar amplification factor, $1 / \left(1 - \frac{C_f}{C_e} \right)$, to the M_f/M_r term of the equation to more accurately represent the maximum moment within the length of the member.

It is clear that Equation 1.10 satisfies the extreme conditions, $C_f = C_r$ when $M_f = 0$

Figure 1.5: Schematic Representation of M_{eq}

and $M_f = M_r$ when $C_f = 0$, and it was found to be conservative in between for members with equal and opposite end moments. However, when the formula was applied to beam-columns with more general end moment conditions, it was found to be too conservative. This conservatism results from the location of the maximum moment, M_{max} . Unlike the case with equal and opposite end moments, M_{max} in general does not occur at midspan of the member. As a result, amplifying the larger end moment by $1 / \left(1 - \frac{C_f}{C_e}\right)$ no longer gives an accurate representation of M_{max} . Therefore, a modification factor, ω , was introduced to the $M_f / M_r \left(1 - \frac{C_f}{C_e}\right)$ term of the equation in order to account for this over-conservatism. The factor ω has a theoretical base, and is explained in Chen and Lui [6], where ωM_f is referred to as an equivalent end moment, M_{eq} , and is such that $\omega M_f / \left(1 - \frac{C_f}{C_e}\right)$ is approximately the maximum moment in the member. This concept is shown schematically in Fig. 1.5.

The code gives an approximate expression for ω , derived by Austin [7], as

$$\omega = 0.6 - 0.4 \frac{M_A}{M_B} \not\leq 0.4 \quad (1.11)$$

where

M_B = Larger end moment

M_A = Smaller end moment

Equation 1.11 is shown in Fig. 1.6 along with the theoretical results for the pin-ended beam-column in the inset of the figure. Clearly, Eq. 1.11 gives a reasonably accurate linear approximation to the theoretical results. It therefore follows from Eq. 1.11 and Fig. 1.5 that $M_{eq} \simeq \omega M_B$ and $M_{max} \simeq \frac{\omega M_B}{1 - \frac{C_f}{C_e}}$ and thus

$$\frac{C_f}{C_r} + \frac{\omega M_f}{M_r \left(1 - \frac{C_f}{C_e}\right)} \leq 1.0 \quad (1.12)$$

is a more general expression than Eq. 1.10.

The Canadian code stipulates that the expression in Eq. 1.11 for ω is only to be used by the designer when he calculates second-order moments (Option a, Section 1.3.1). When he calculates linear moments (Option b), the code requires him to use $\omega = 0.85$ for double curvature and $\omega = 1.0$ for single curvature. These values were suggested by the 1963 American Institute of Steel Construction (AISC) code which was said to result in a conservative design [8]. It is clear, though, that these restrictions cannot possibly cover all cases to be encountered by the designer. Therefore, it is conceivable that a non-conservative design could result through their use.

1.3.4 Column Effective Length

The effective length of a column is known for ideal, simple end conditions (fixed, pinned, or free). However, for more practical end conditions, the effective length has to be approximated. The Canadian code provides the engineer with two options for approximating

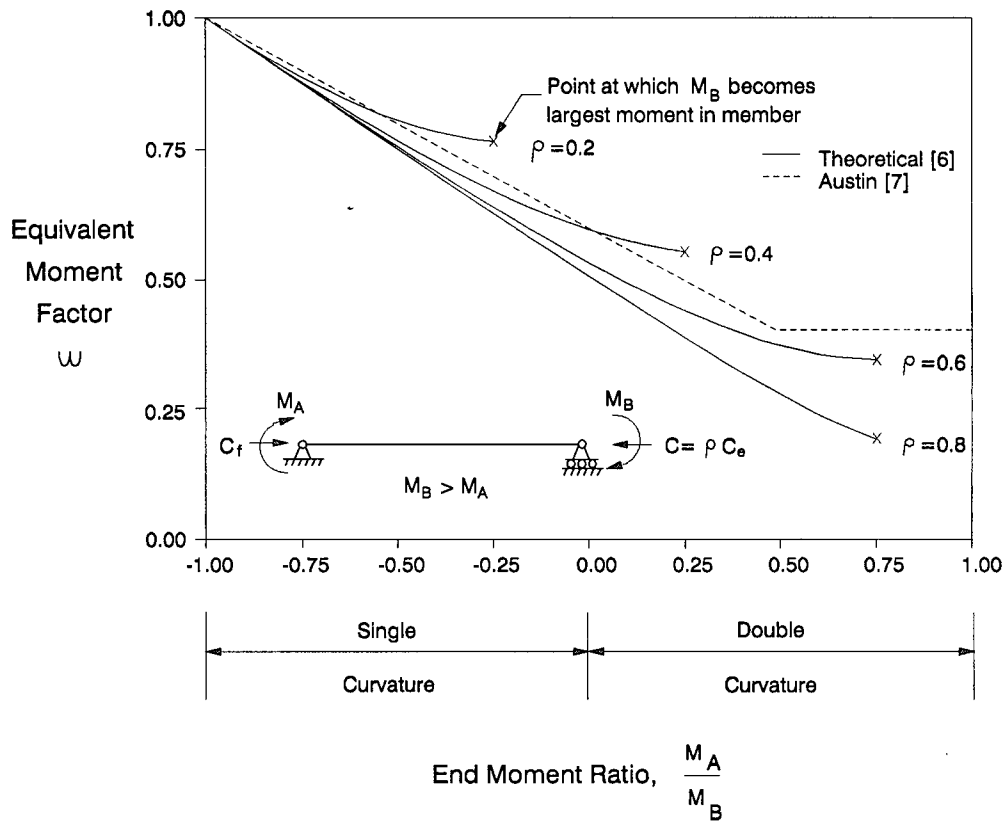


Figure 1.6: Theoretical and Approximate Equivalent Moment Factor, ω

the effective length, “side-sway prevented” and “side-sway permitted”, based on more complex ideal end conditions.

Side-Sway Prevented

The governing differential equation for the idealized sway-prevented column in Fig. 1.7b is:

$$EI \frac{d^4 y}{dx^4} + C \frac{d^2 y}{dx^2} = 0 \quad (1.13)$$

with the boundary conditions:

$$\begin{aligned} y(0) &= 0 \\ y(L) &= 0 \\ M(0) &= k_l \theta_l \\ M(L) &= k_u \theta_u \end{aligned} \quad (1.14)$$

where:

$$\theta_l = \frac{dy(0)}{dx}$$

$$\theta_u = -\frac{dy(L)}{dx}$$

k_u, k_l = Joint rotational spring constants

The rotational resistance, k_u and k_l , is provided to the column by the girders framing into the upper and lower joints respectively. If one assumes that all of the columns in the structure buckle at the same time, and that the resistance to rotation of all members is proportional to their stiffness, I/L , the resisting moment, M_u , acting on the column in Fig. 1.7 will be:

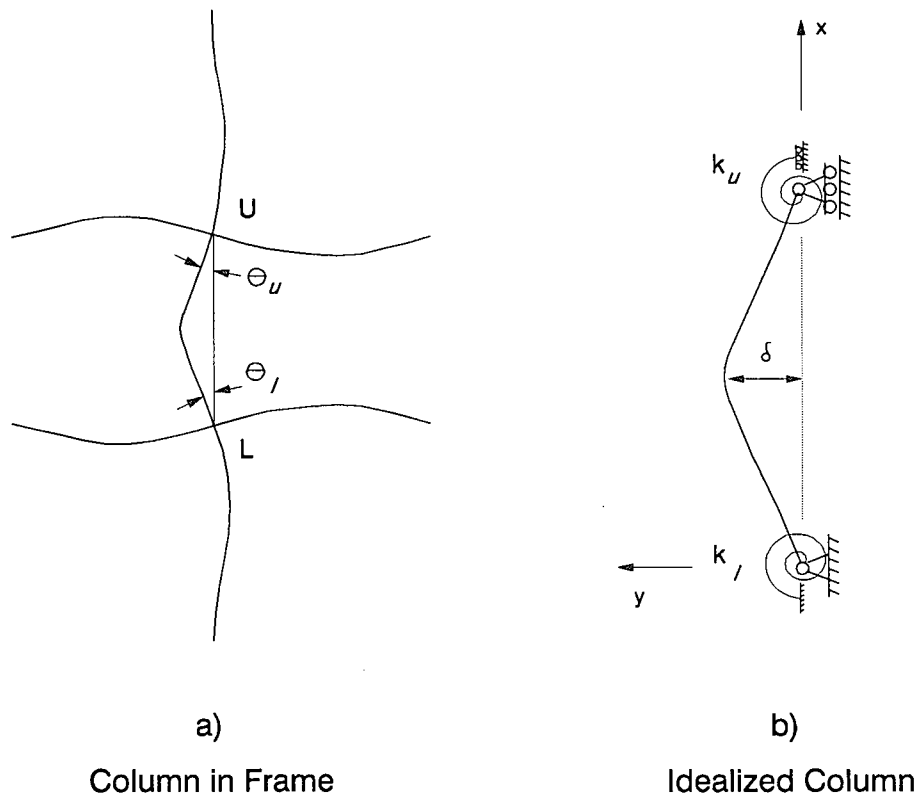


Figure 1.7: Sway-Prevented Column

$$M_u = \frac{\frac{I_c}{L_c}}{\sum \left(\frac{I_c}{L_c}\right)_u} 2E\theta_u \sum \left(\frac{I_g}{L_g}\right)_u = \frac{2EI_c}{G_u L_c} \theta_u \quad (1.15)$$

$$\text{where } G_u = \frac{\sum \left(\frac{I_c}{L_c}\right)_u}{\sum \left(\frac{I_g}{L_g}\right)_u}$$

Clearly, the expression for M_l is the same as Eq. 1.15, with the u subscripts replaced by l subscripts.

Thus the solution to Eq. 1.13 can be expressed as:

$$\frac{G_u G_l}{4} \left(\frac{\pi}{k}\right)^2 + \left(\frac{G_u + G_l}{2}\right) \left(1 - \frac{\frac{\pi}{k}}{\tan \frac{\pi}{k}}\right) + 2 \frac{\tan \frac{\pi}{2k}}{\frac{\pi}{k}} = 1.0 \quad (1.16)$$

where:

k = Effective length factor of the column under consideration

This equation has been conveniently put in the form of a nomograph (sway-prevented) which can be found in the Canadian code.

Side-Sway Permitted

The governing differential equation for the idealized sway-permitted column in Fig. 1.8 b is the same as Eq. 1.13. However, the boundary conditions differ from those of Eq. 1.14 and are:

$$\begin{aligned} y(0) &= 0 \\ V(L) &= 0 \\ M(0) &= k_l \theta_l \\ M(L) &= k_u \theta_u \end{aligned} \quad (1.17)$$

and the resulting resisting moment, M_u , acting on the column will be:

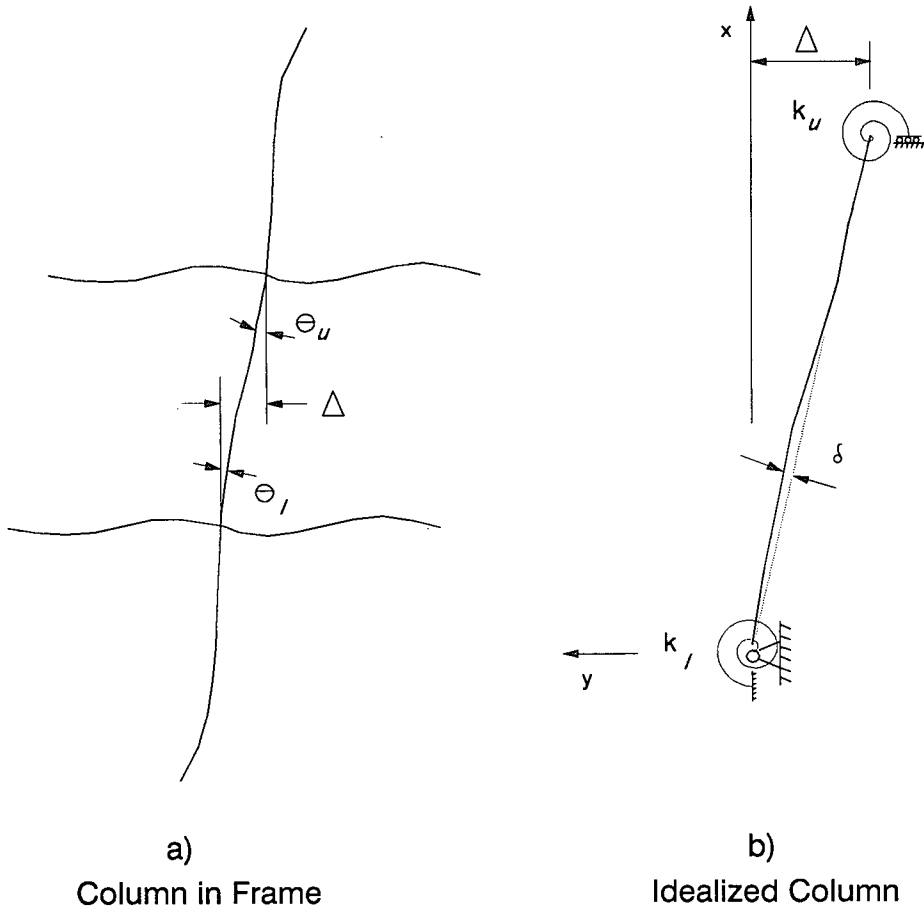


Figure 1.8: Sway-Permitted Column

$$M_u = \frac{6EI_c}{G_u L_c} \theta_u \quad (1.18)$$

and similarly for M_l . Furthermore, the solution to eq. 1.13 can be expressed as:

$$\frac{G_u G_l \left(\frac{\pi}{k}\right)^2 - 36}{6(G_u + G_l)} = \frac{\pi k}{\tan \frac{\pi}{k}} \quad (1.19)$$

This equation has also been put in the form of a nomograph (sway-permitted).

The main distinction between the sway-prevented model and the sway-permitted model is that the deformed shape of the sway column gives rise to an additional $C\Delta$ moment. This is over and above the $C\delta$ moment of the nonsway column (see Fig. 1.8 for the definition of Δ and δ). This $C\Delta$ moment must be resisted by the bending action of the girders and columns under consideration. Thus, if the $C\Delta$ moments are not included in the analysis procedure, i.e. linear moments, the side-sway permitted model is used for approximating the effective length. If, however, the $C\Delta$ moments are included in the analysis procedure, i.e. second order moments, the sway prevented model is used in order to account only for the $C\delta$ moments.

1.3.5 Limit of Application

The types of structures that the Canadian code is applicable to is limited to rigidly connected frames in which all of the columns reach their critical buckling load simultaneously. The major cause of this strict limitation is found in the derivation of the column effective length factor, k , used in the design equations, Eqs. 1.3 to 1.5. When deriving the expressions for k , it was assumed that there was no support provided to one column by another. Clearly, this will rarely occur in practice. It is true that when the column being designed is supported by another column, the resulting design should be conservative. However, it is unconservative with respect to the supporting column as the

code equations do not take into account the additional forces that arise in it.

Further, in the derivation of k , the code assumes that the girders framing into the column help the column resist the second-order ($C\Delta$) moments. However, when designing the girders, forces caused by such assistance are ignored. That is, by separating the design of the beam columns and the girders, the code allows for a non-conservative design of the girders. This is an example of a member that carries no axial load, yet has a moment amplification factor. This problem is alleviated through the use of a second-order analysis.

There are also problems with some of the approximations illustrated in the previous sections. One of the more serious problems arises when using the equivalent moment factor, ω , as given by Eq. 1.11. It has been found that this expression can give erratic results for members with double curvature, while it gives adequate results for members bent in single curvature [4].

Also, when using a linear analysis, the limitations on ω of 1.0 for single curvature and 0.85 for double curvature as described in Sec. 1.3.3, combined with the fact that the moments used in the design equations are the linear rather than the true second-order moments, ensures that the second strength equation, Eq. 1.4, never governs the design. This is unfortunate, as it is one of the two design equations that has a theoretical base.

1.4 The 1986 American Steel Code

The 1986 American Load and Resistance Factored Design (LRFD) Steel code is very similar to the Canadian code described in Section 1.3. It is the first American steel code to use the probability based limit states design method, as previous editions have employed the working stress design method. The load factors, though, are slightly different from the Canadian load factors, in an effort to more accurately represent actual conditions in the U.S..

This code has made an attempt to eliminate many of the limitations and shortcomings found in the Canadian code. Perhaps the most significant difference is that the maximum moment in the stability equation, Eq. 1.5, can not be less than the maximum end moment, which is currently permitted by the Canadian code. This limitation eliminates the need for the strength equations, Eq. 1.3 and Eq. 1.4, as they no longer govern.

The stability equation has been altered slightly from eq. 1.5 in the Canadian code, and is as follows:

$$\frac{C_f}{\phi_c C_n} + \frac{8M_f}{9\phi_b M_n} \leq 1.0 \quad \frac{C_f}{\phi_c C_n} \geq 0.2 \quad (1.20)$$

$$\frac{C_f}{2\phi_c C_n} + \frac{M_f}{\phi_b M_n} \leq 1.0 \quad \frac{C_f}{\phi_c C_n} < 0.2 \quad (1.21)$$

where:

C_f = Axial compression in the member due to factored loads

C_n = Nominal compressive strength, = $f \left(\frac{kL}{r} \right)$, see eq. 1.22

M_f = Bending moment in the member due to factored loads (see below)

M_n = Nominal flexural strength

ϕ_c = resistance factor in compression = 0.85

ϕ_b = resistance factor in flexure = 0.90

Equations 1.20 and 1.21 represent a continuous function as shown in Fig. 1.9. It should be noted that Fig. 1.9 looks very similar to the yield surface of the Canadian code, Fig. 1.2. However, Fig. 1.9 has substantially different variables along the axes, C_f/C_n along the x-axis and M_f/M_n along the y-axis, while Fig. 1.2 has C_f/C_y and M_f/M_p respectively. Thus, the resulting “failure surface” is different.

The expression for C_n is similar to that of C_r in the Canadian code, though C_n is less complex.

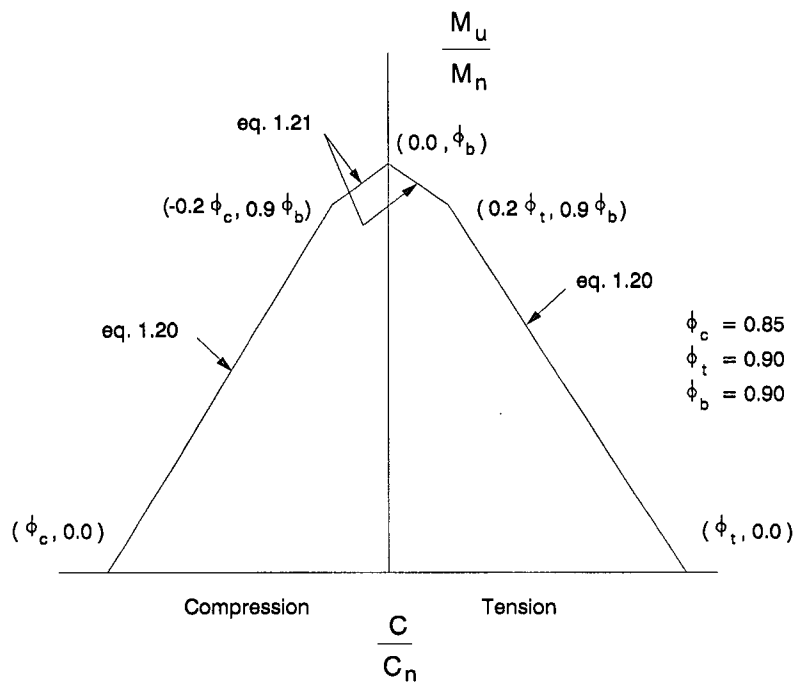


Figure 1.9: American Moment-Axial Failure Surface

$$\begin{aligned}
C_n &= (0.658\lambda^2) C_y \quad \lambda \leq 1.5 \\
C_n &= \left(\frac{0.877}{\lambda^2}\right) C_y \quad \lambda > 1.5
\end{aligned}
\tag{1.22}$$

where the nomenclature is the same as in Eq. 1.6.

The expression for M_n is more complex than that of M_r in the Canadian code, however for laterally supported members, both reduce to M_p , the plastic moment.

As with the Canadian code, the designer has the option of using a second order or linear analysis to determine the member forces. The maximum moment in the beam-column, M_f , used in Eqs. 1.20 and 1.21 can be found through the use of a second-order analysis, or the use of a linear analysis combined with the following equation:

$$M_f = B_1 M_{nt} + B_2 M_{lt} \tag{1.23}$$

where:

M_{nt} = Linear moment in member assuming there is no lateral translation of the frame

M_{lt} = Linear moment in member as a result of lateral translation of the frame only

$$B_1 = \frac{\omega}{1 - \frac{C_f}{C_e}} \not\leq 1.0$$

$C_e = C_y / \lambda^2$ where λ is determined with $k \leq 1.0$

$\omega = 0.6 - 0.4 \frac{M_A}{M_B}$ for members in braced frames

= 0.85 for members with restrained ends in sway frames

= 1.0 for members with unrestrained ends in sway frames

$$B_2 = \frac{1}{1 - \sum C_f \left(\frac{\Delta_{oh}}{\sum H_f L} \right)}$$

$$\text{or} = \frac{1}{1 - \frac{\sum C_f}{\sum C_e}}$$

$\sum C_f$ = Sum of axial loads in all columns in a storey

Δ_{oh} = Linear translation deflection of storey under consideration

$\sum H_f$ = Sum of storey horizontal forces causing Δ_{oh}

L = Storey height

$\sum C_e$ = Sum of storey columns Euler loads, each with $k \geq 1.0$

Note that there is no limit of 0.4 on ω that there is in the Canadian formulation. Also, C_e in the expression for B_1 uses $k \geq 1.0$, while in the expression for B_2 , C_e uses $k \leq 1.0$. In Equation 1.23, $B_1 M_{lt}$ is an approximation for the moment caused by gravity loads, while $B_2 M_{lt}$ is an approximation for the moment caused by sidesway loads. The sum of the two gives a conservative estimate for M_{max} as they do not necessarily occur at the same location in the member. Also notice that, unlike the Canadian code, the value of C_n used in Eqs. 1.20 and 1.21 is the same regardless of whether the designer calculates linear or second-order moments. This, combined with the fact that the expression for B_2 takes into account the differing axial loads in adjacent columns of the same storey (ie. the columns helping one another is included) results in very similar linear and second-order designs. The Canadian second-order design, on the other hand, generally allows for much more load carrying capacity than does the linear design. The result of this is that the Canadian designer is rewarded for carrying out the more refined second-order design, while the American designer receives no such incentive.

It should be noted that the American calculation of P_n is based on the sway permitted effective length factor for both the linear and second order designs. This is contrary to the Canadian procedure.

Chapter 2

An Alternative Design Method

2.1 General

More powerful, less expensive computer hardware and more sophisticated computer software allow the design engineer to carry out both the design and analysis of a structure simultaneously. This is unlike present design methods, which require the analysis to be followed by a series of code checks.

Current design codes have the engineer choose a preliminary structure and analyze it linear elastically with a computer program to obtain the member moments and axial forces. These forces are then used in the code equations to decide whether the members are satisfactory. If the members are satisfactory, the designer has a choice. He can reduce the size of some or all of the members and repeat the design, or he can accept the members, at which point the design is finished. If, however, the members are not satisfactory, he must increase the size of some or all the members, rerun the analysis, and decide whether the new members are satisfactory. This process continues until the designer is satisfied with the structure. Clearly, unless the designer is very skilled or very lucky, this process can take a great deal of time.

A much faster, more efficient design method, however, is available to the engineer. Rather than using a linear elastic computer program to analyze the structure, the designer can use a second-order program that includes both nonlinear material properties (i.e. plastic hinges), nonlinear geometric properties (i.e. equilibrium calculated on the deflected

shape), moment-axial interaction (yield surface), and stability effects. With a program of this type, the designer chooses a preliminary structure and analyzes it until yielding first occurs. If the applied loads at this point are greater than the factored loads the designer chooses to either reduce the size of some or all of the members, or leave them unaltered in which case the design is finished. If, however the loads are less than those required, the designer must increase the size of some of the members (usually near the location of the first hinge) and reruns the program until the loads are greater than those required. The obvious time saving advantage of this method is that it “bypasses” the code checks.

There are many such computer programs commercially available. The program used in this work is ULA (Ultimate Load Analysis) [9] which runs on an IBM personal computer (PC, XT, AT, PS2), or compatible. ULA was chosen as it was readily available at the University of British Columbia.

2.2 ULA Theory and Underlying Assumptions

ULA is a plane frame stiffness program which combines second-order analysis with plastic hinge formation, stability effects and moment-axial interaction. It is an interactive program that uses GKS graphics. This allows the user to monitor the structure on the screen and to place plastic hinges when necessary as the load is increased to ultimate.

As is commonly practiced with the limit states design method described in Section 1.1, ULA allows for load vectors as follows

$$F = \alpha_1 F_1 + \alpha_2 F_2 + \alpha_3 F_3 + \dots \quad (2.24)$$

where F is a linear combination of load cases F_i , eg. dead load, live load, etc., factored by the appropriate load factor α_i . ULA accomplishes this by separating the load vector

into two part, as follows:

$$F = F_D + \lambda \bar{F} \quad (2.25)$$

where F_D is a constant component of the load vector and \bar{F} is a variable component factored by the load level λ . In this way, a portion of the load, for example the dead load, can be placed on the structure and held constant while the remainder of the load, for example the live load, can be increased until collapse.

2.2.1 Second-Order Elasto-Plastic Analysis with Moment-Axial Interaction

ULA uses a simple combination of several well established structural theories. The user increases the load level λ incrementally, and at each load level equilibrium is calculated on the deformed shape. This is achieved by using stability functions in the member matrix, the details of which will not be discussed here as they are standard and have been presented by many authors including Gere and Weaver [10]. It should, however, be noted that the stability functions depend on the member axial forces, and the axial forces depend on the deflected shape. Therefore, it is necessary to iterate towards a solution at each load level. This is handled by ULA with its interactive format as the user can view both the determinant of the structure stiffness matrix and the joint deflections converge. Generally, two cycles are enough for convergence for small, stiff structures. However, for larger, more flexible structures or stiff structures with several plastic hinges, the number of cycles to convergence is often greater than two.

The load level is increased by the user until the moment capacity of a member is reached. ULA allows for the reduction of moment carrying capacity of a member due to axial load through a moment-axial interaction surface, or yield surface. As was illustrated in Section 1.3.2 for an I-shaped section, each structural section has its own yield surface.

For a given section, the yield surface can be approximated by a series of straight lines or facets. The yield surface is input to ULA by the intersection points of these facets. ULA allows only symmetric sections and therefore requires the input of only the top half of the yield surface.

The yield surface used throughout this work is shown in Fig. 2.10 and is the same as that specified by CAN3-S16.1-M84 for I-shaped sections, Fig. 1.3, with $\phi = 1.0$. A plastic hinge forms when the combination of moment and axial force is sufficient to reach the yield surface. ULA defines a parameter φ_i for each facet such that when $\varphi_i = 1$, the yield surface has been reached and a hinge should be placed. The parameter φ_i is defined as follows:

$$\varphi_i = \frac{m}{b_i} + \frac{p}{a_i} \quad (2.26)$$

where $m = |M|/M_p = |M|/\sigma_y Z$, $p = C/C_y = C/\sigma_y A$ and a_i and b_i are the intercepts of each facet with the p and m axis respectively.

The convenience of the interactive format in ULA now becomes apparent. At each load level, once the second order convergence is achieved, a plot of the structure appears on the screen with a list of the five maximum φ_i values and their locations on the structure. ULA offers the user an estimate of the load level at which the next hinge will form. This is accomplished by linearly extrapolating between two known points within the yield surface and the surface itself. The basic assumptions in this estimation are that line 1-2-H in Fig. 2.10 is straight and that p is linear with λ .

When a plastic hinge is placed at the end of a member, ULA adds another joint, known as a slave joint, at the hinge location which has the same translation as the master joint, but a different rotation. The load vector F is then increased in size by one, and a moment, equal to the moment capacity of the member, $\pm M_{pc}$, is added to the

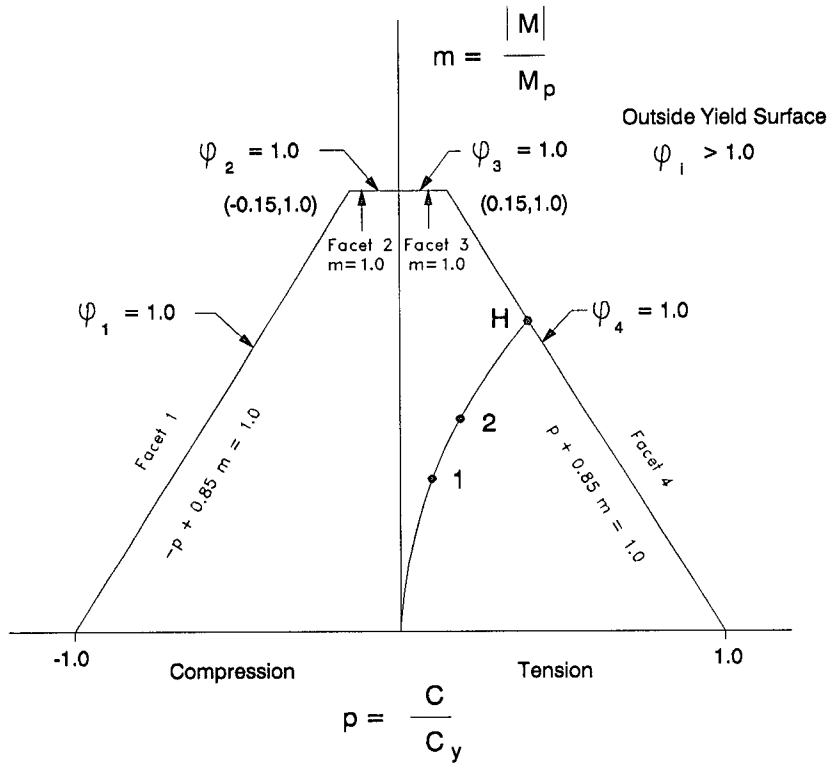


Figure 2.10: Moment-Axial Failure Surface Used in ULA

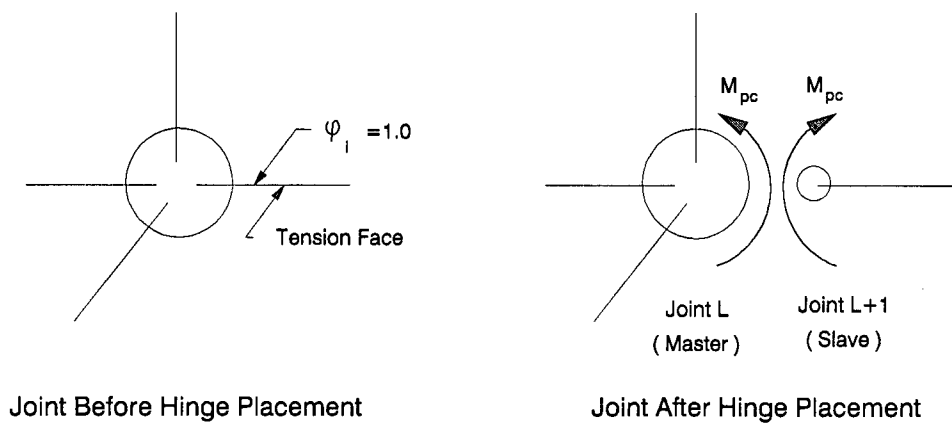


Figure 2.11: Joint Before and After Hinge Placement

slave and master rotational degrees of freedom as shown in Fig. 2.11. Thus the new load vector becomes $F = F_D + \lambda \bar{F} + F_p$ where F_p contains only $\pm M_{pc}$. It should also be noted that once the hinge has been placed, the values of M_{pc} are updated at higher load levels to reflect the change in member axial forces.

After the first hinge is placed, ULA also changes the structure stiffness matrix to include the extra rotational degree of freedom of the slave joint, and proceeds with the analysis until one of two things happens. Either the structure is now unstable, in which case ULA plots the mechanism on the screen, or the user increases the load level until the moment capacity of another member is reached. At this point, the user places the next hinge and the procedure is repeated until the structure reaches instability, signified by the determinant of the structure stiffness matrix going to zero.

This entire sequence is shown for a single bay frame in Fig. 2.12 and the corresponding response versus load level is shown in Fig. 2.13.

It is important to note that each of the structures in Fig. 2.12 is only valid for a specific range of λ . Each structure has its own stiffness matrix and each will be analyzed

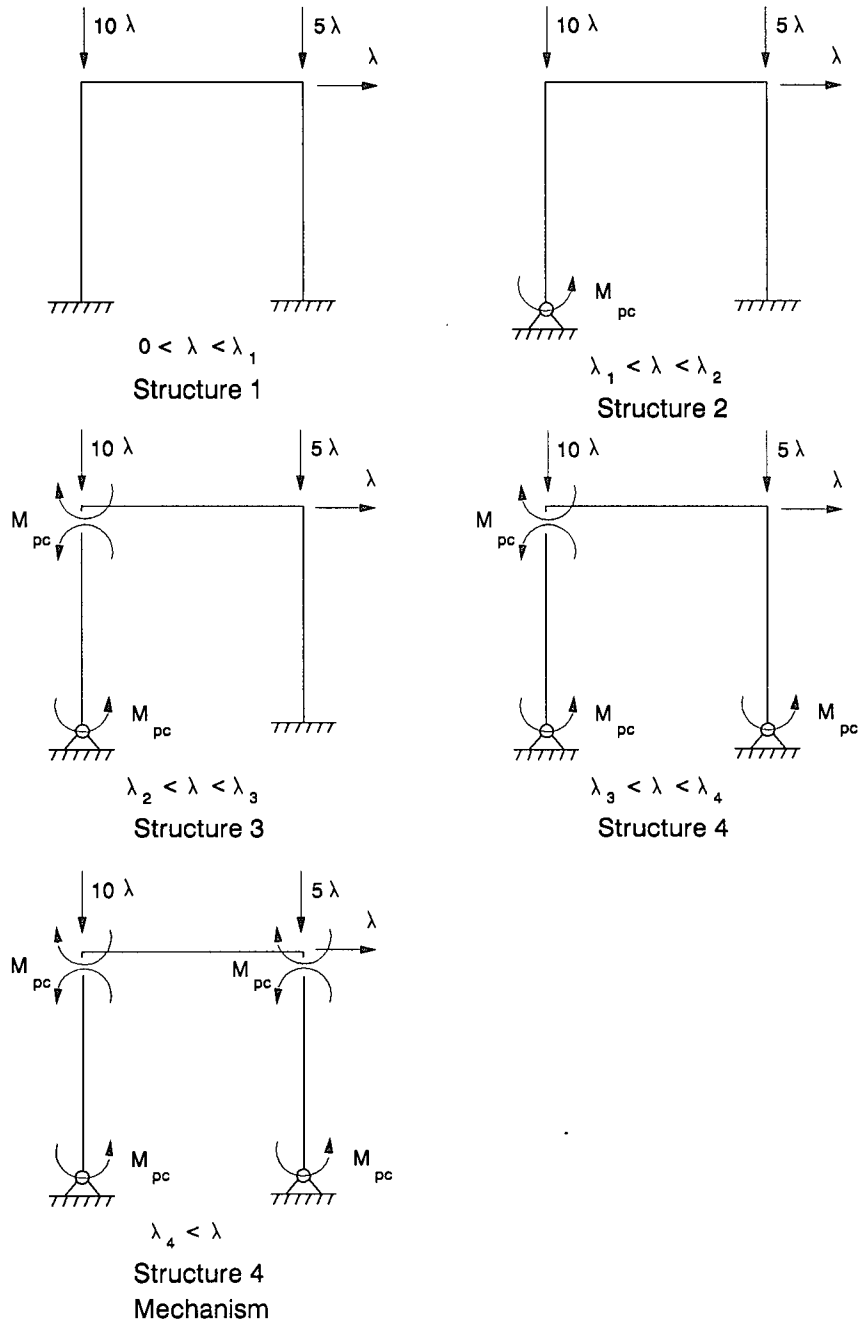


Figure 2.12: Hinge Formation Sequence

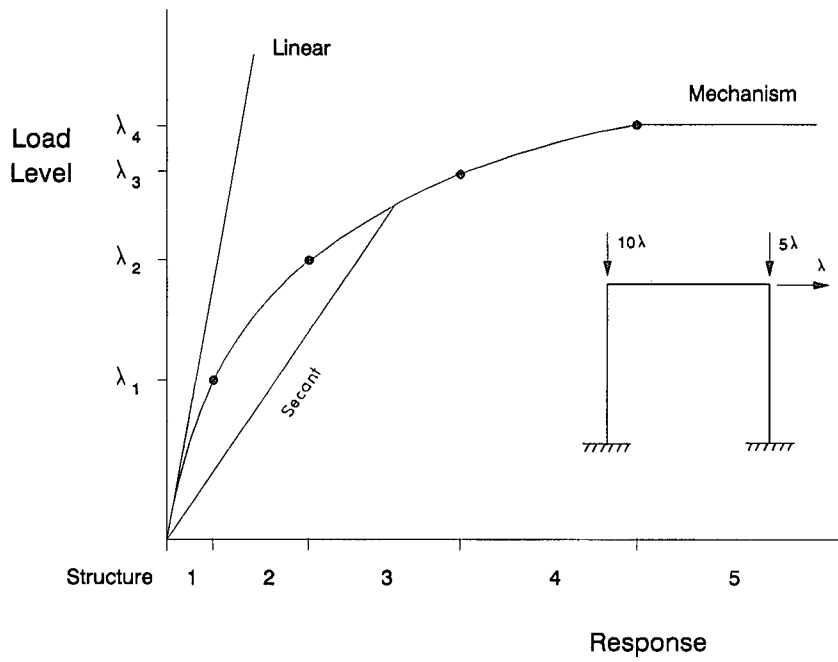


Figure 2.13: Second-Order Elasto-Plastic Response

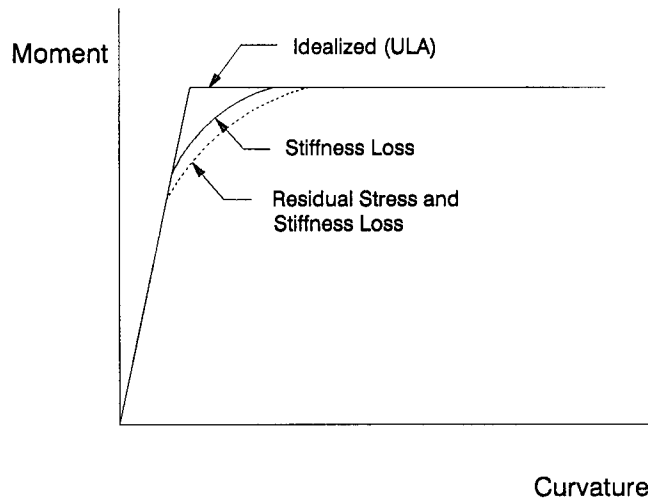


Figure 2.14: Idealized Elasto-Plastic Behaviour

under the loads shown.

2.2.2 Moment Curvature

A perfect elasto-plastic material is assumed by ULA as shown in Fig. 2.14. Also included in Fig. 2.14 is a relationship that includes the effect of stiffness loss due to yielding, and another that includes the effects of stiffness loss and residual stresses. These two effects are neglected in ULA and therefore are neglected in this work.

The effect of this assumption varies with axial load. However, work has been done by Galambos and Ketter [11] and their findings, based on the assumed residual stress pattern shown in Fig. 2.16, are shown in Fig. 2.15. The expressions used for the residual tension stress, σ_{RT} , and the residual compressive stress, σ_{RC} , are shown in Fig. 2.16.

The errors incurred by assuming a perfectly elasto-plastic behaviour are nonconservative. However, with increased curvature the error between the assumed and the real behaviour decreases. As a result, the error is a local one and the error from most of the

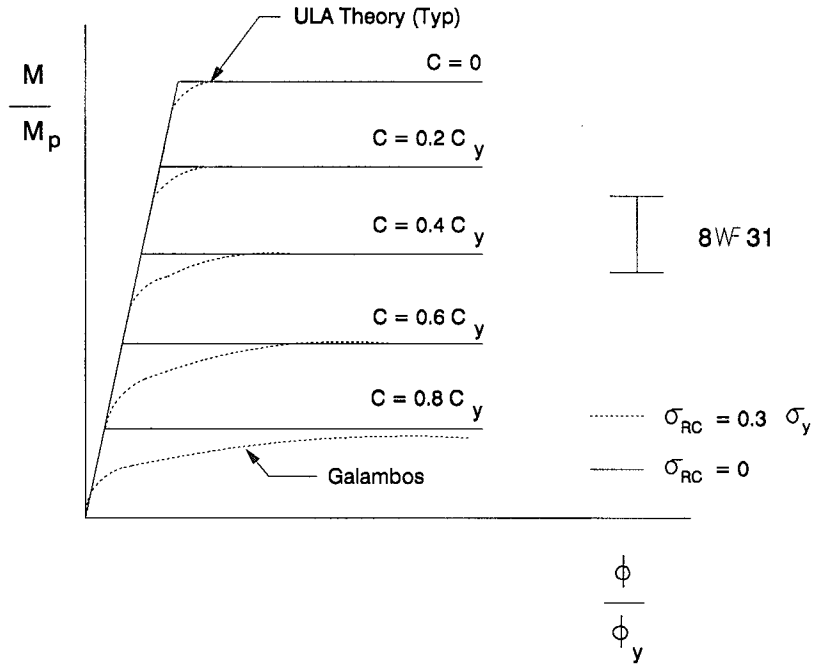


Figure 2.15: Moment-Axial-Curvature Relationship

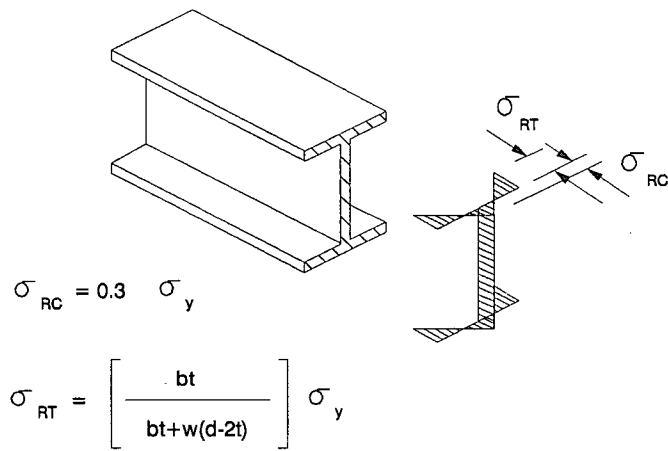


Figure 2.16: Cooling Residual Stress Pattern

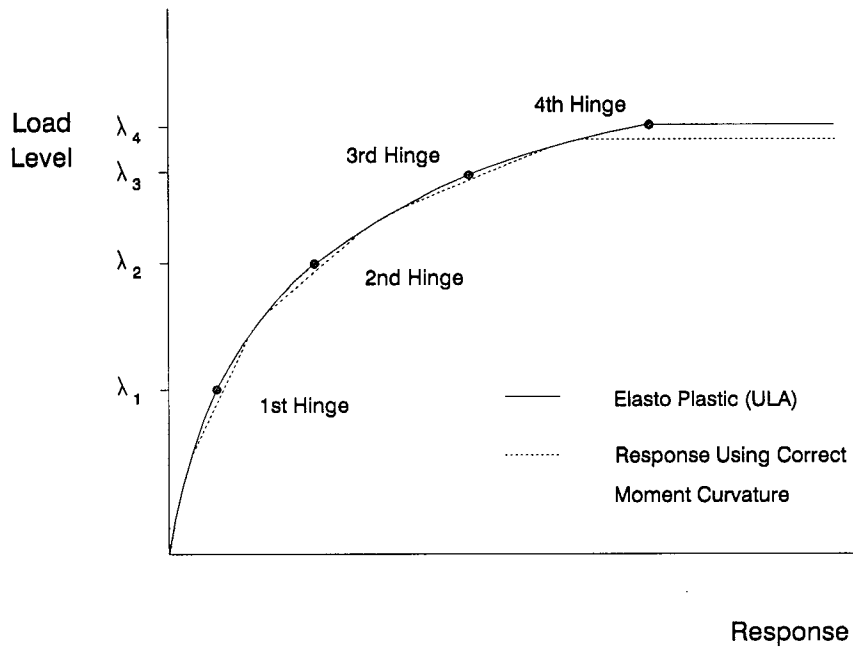


Figure 2.17: Effect of Elasto-Plastic Assumption

hinges formed prior to collapse will not affect the ultimate load. Any non-conservatism should only occur due to the last hinge formed, as demonstrated in Fig. 2.17. It is therefore proposed that the effect of idealizing the behaviour as perfectly elasto-plastic is not too significant, perhaps as much as 10%.

The program ULA, with its interactive graphics format gives the user a complete and quickly understood appreciation of how a particular structure is behaving with increasing load level, and where it may need redesign or where material is not being used efficiently.

Chapter 3

Verification of ULA

3.1 General

It is the intention of this chapter to verify the accuracy of the computer program ULA. The program will be used to develop a modified load versus L/r curve for the pin ended column shown in Fig. 3.18. Note that the column is modelled as two straight members, with three joints, with the middle joint having an initial eccentricity chosen to be $L/1000$. This value was selected to represent the maximum fabrication eccentricity of a steel column. Also, ULA requires a “driving force” for hinge formation and without some eccentricity, the program would give a perfect plastic-Euler curve. The results obtained from ULA for this column are expected to be slightly nonconservative due to the perfect elasto-plastic assumption of Section 2.2.2. This column curve will then be compared to the Canadian code, the American code, and the curve given by the Column Research Council (CRC) [12]. Also, two full sized test frames will be analyzed with ULA, and the results will be compared to the experimental results.

3.2 A Centrally Loaded, Initially Eccentric Column

3.2.1 Governing Parameters

The ultimate column capacity, C_u , of the column shown in Fig. 3.18 is a function of the following six independent parameters:

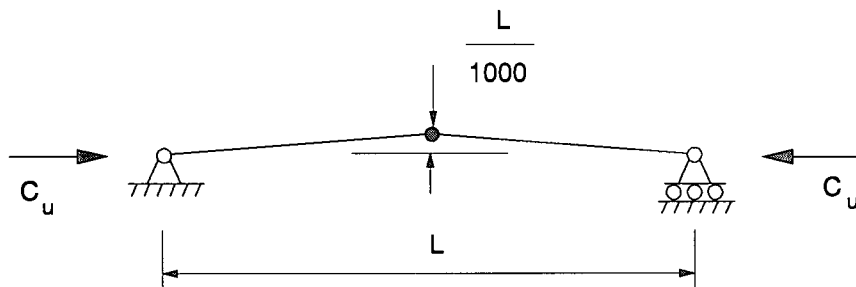


Figure 3.18: Pin Ended Column Used in the Computer Analysis

$$C_u = f \{L, EI, AE, M_p, C_y, e_0\} \quad (3.27)$$

where:

L = column length

EI = linear elastic bending stiffness

AE = linear elastic axial stiffness

$M_p = Z\sigma_y$ = maximum possible bending moment with no axial load present

$C_y = A\sigma_y$ = maximum possible axial load with no moment present

σ_y = yield stress

e_0 = initial midspan eccentricity

With several independent variables, it is convenient to use the Buckingham II Theorem to reduce the number of governing parameters. With seven variables in Eq. 3.27 dependent on the two dimensions of force and length, only five dimensionless groups are required to describe the system as follows:

$$\frac{C_u}{C_y} = f \left\{ \sqrt{\frac{C_y L^2}{\pi^2 EI}}, \frac{e_0}{L}, \frac{M_p/C_y}{\sqrt{EI/AE}}, \frac{C_y}{AE} \right\} \quad (3.28)$$

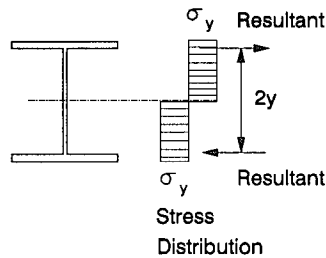
The seemingly awkward ratios of eq. 3.28 were carefully chosen in order to simplify to the more familiar ratios shown below:

$$\frac{C_u}{C_y} = f \left\{ \lambda, \frac{e_0}{L}, \frac{y}{r}, \epsilon_y \right\} \quad (3.29)$$

where:

$\lambda = \frac{kL}{r} \sqrt{\frac{\sigma_y}{\pi^2 E}}$ = the modified L/r II group used by the codes

y = the distance from the centre of gravity of a symmetric section to the centre of gravity of either the upper or lower half



$r = \sqrt{\frac{I}{A}} = \sqrt{\frac{EI}{AE}}$ = radius of gyration

$\epsilon_y = \frac{\sigma_y}{E} = \frac{C_y}{AE}$ = yield strain

3.2.2 Variation of Parameters

For comparison purposes with the codes and the CRC curve, C_u/C_y was plotted against λ for various y/r and ϵ_y values. It was decided that a value of 1/1000 to represent the maximum fabrication eccentricity was acceptable for e_0/L , and thus it was not changed.

The values of y/r were calculated for all W-shapes provided by the Canadian code. It was found that the parameter varied between 0.90 and 0.96. Thus values for y/r of 0.90 and 0.96 were used with a value of 0.0015 for ϵ_y , and the results are shown in Fig. 3.19.

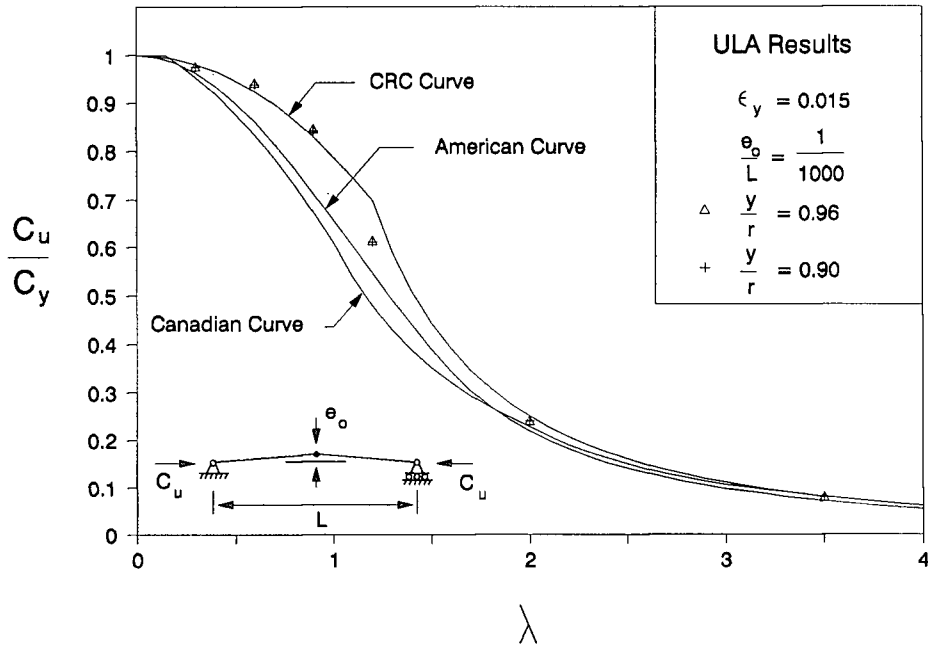
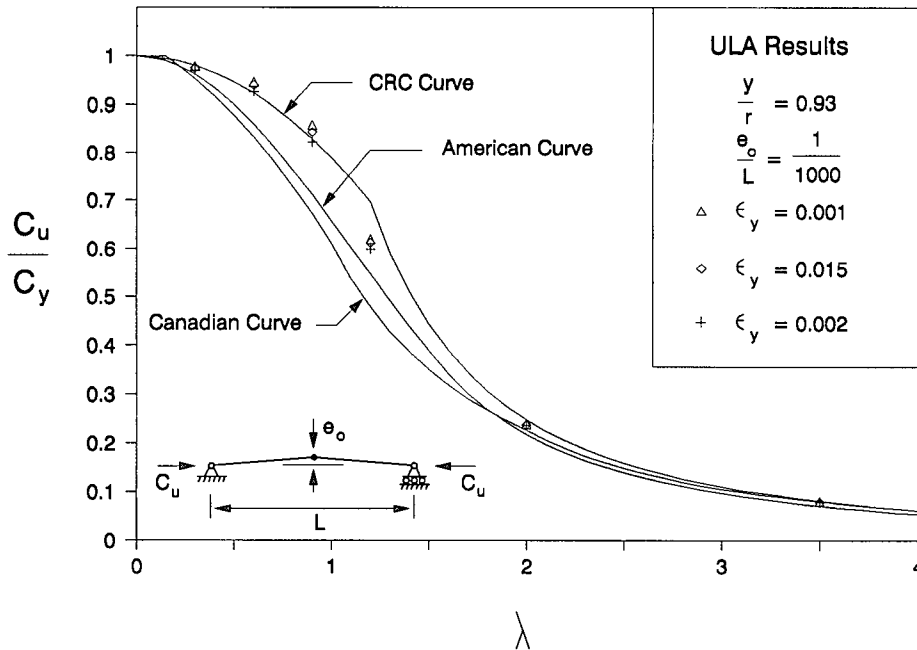


Figure 3.19: Variation of y/r for a Simple Column

Figure 3.20: Variation of ϵ_y for a Simple Column

The value of ϵ_y for normal steel varies from approximately 0.001 to 0.002 ($\sigma_y = 30$ to 60 ksi, 200 to 400 MPa). Values for ϵ_y of 0.001, 0.0015, and 0.002 were used with a value of 0.93 for y/r and the results are shown in Fig. 3.20.

It is apparent from Fig. 3.19 that the parameter y/r has very little effect on the ultimate strength parameter C_u/C_y . Therefore, a value of $y/r = 0.93$ will be used in the remainder of this work. The variation of ϵ_y has a slightly larger effect; however, for comparison purposes, a value of $\epsilon_y = 0.0015$ will be used in the remainder of this work.

Both Fig. 3.19 and Fig. 3.20 include the Canadian code, the American code, and the CRC curves. The Canadian and American curves have been modified slightly from Equations 1.6 and 1.22 respectively, to compare more correctly with the analytical results of ULA. The factor $\phi = 0.9$ has been removed from the Canadian curve, and the factor

$\phi = 0.85$ has been removed from the American curve. Note that the two curves can not be correctly compared to each other in the form presented here as the respective codes use different ϕ factors. The CRC curve is as follows:

$$\begin{aligned} \frac{C_u}{C_y} &= 1.0 - 0.21\lambda^2 & 0 \leq \lambda \leq 1.2 \\ \frac{C_u}{C_y} &= \lambda^{-2} & 1.2 < \lambda \end{aligned} \quad (3.30)$$

and has been developed using the tangent modulus theory combined with the assumed residual stress pattern of fig. 2.16. Because ULA neglects residual stresses completely, it is somewhat surprising to see that the CRC curve and the results from ULA compare so well in fig. 3.19 and fig. 3.20. As expected, ULA does give consistently higher results than both the codes due to the built in conservatism of the latter. The results, however, are considered to be very acceptable.

3.3 Yaramci Test Frame B

In 1966 Erol Yaramci performed experimental tests on three steel frames at Lehigh University as part of his Ph.D. thesis [13]. The results of one of his tests, test frame B, are reproduced in Fig. 3.21. Also shown in the figure are Yaramci's analytical results and the analytical results from ULA, both of which neglected strain hardening. The frame itself is shown in the inset of Fig. 3.21. All of the analytical work used the measured EI and M_p values, rather than the handbook values, to more accurately compare with the experimental test. These values are shown in Table 3.1.

Clearly all the results coincide in the elastic range, and then deviate from one another after the first hinge forms. Even with these differences, though, the ultimate load from ULA is only 10% higher than the experiment. In his thesis, Yaramci does explain why his

Member	Section	Measured EI <i>kip - in.²</i>	Measured M_p <i>kip - in.</i>	Handbook EI <i>kip - in.²</i>	Handbook M_p <i>kip - in.</i>
Columns	5 M 18.9	400×10^4	1100	400×10^4	1060
Beams	10 WF 25	73×10^4	400	70×10^4	394

Table 3.1: Measured Values For Yaramci Test Frame B

analytical results are even higher, and thus this thesis will not be concerned with this. The results from ULA are high as expected, as the perfectly elasto-plastic assumption and the perfectly rigid connections at the base of the frame assumed by ULA are unconservative. However, 10% error is considered acceptable by the author.

3.4 Baker Pin-Based Test Frame

In 1952, Professor J. Baker published a paper in the U.K. [14] in which he described destructive tests of several welded portal frames constructed of 8-inch by 4-inch joist sections. The results from one of the pin-based frames are reproduced in Fig. 3.22 along with the analytical results from ULA. The test frame is a single bay rectangular frame and is shown in the inset of Fig. 3.22. Unlike Yaramci, Baker did not measure the EI and M_p values of the sections, nor did he measure the yield stress of the members directly. He did select two members from the same batch of material as those used in the construction of the frame, and tested these members as simply supported beams. From these two tests, a “minimum average yield stress” for the members was quoted as 16.9 tons per square inch (33.8 ksi, 230 MPa). This value of σ_y was used in ULA along with I and Z values obtained from the British Standards [15] for an 8-inch by 4-inch joist section. Furthermore, the exact dimensions of the frame were not specified in the paper. The span was given as $15' - 11\frac{1}{8}''$ (4855 mm), however, the height of the frame

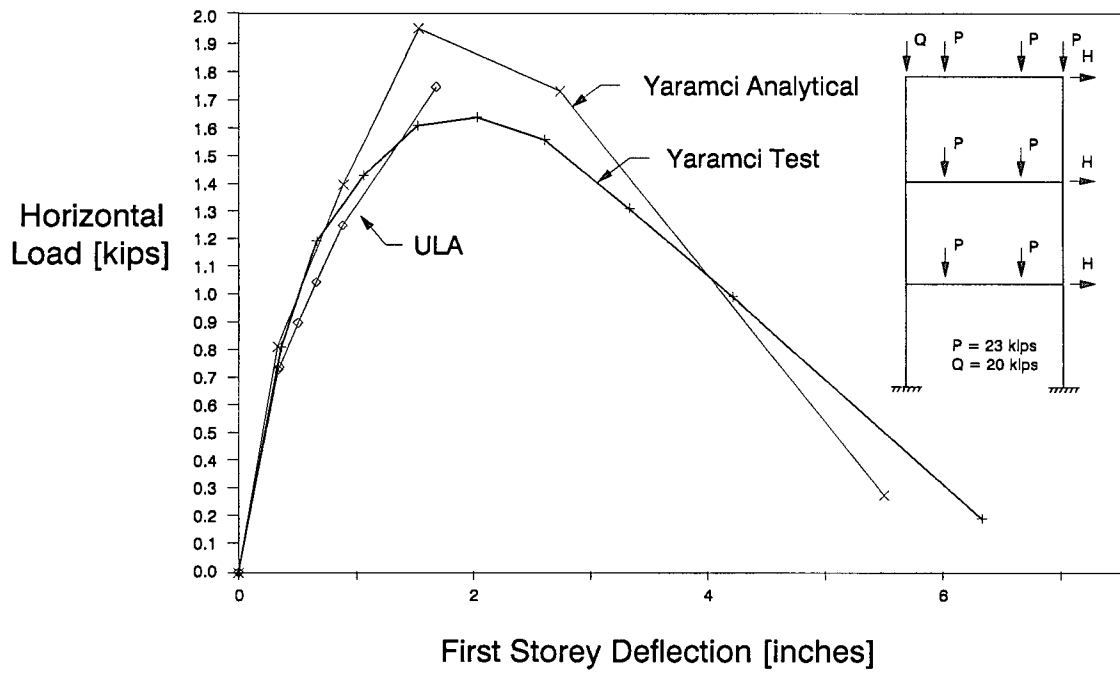


Figure 3.21: Load-Deflection Curves for Yaramci Test Frame B

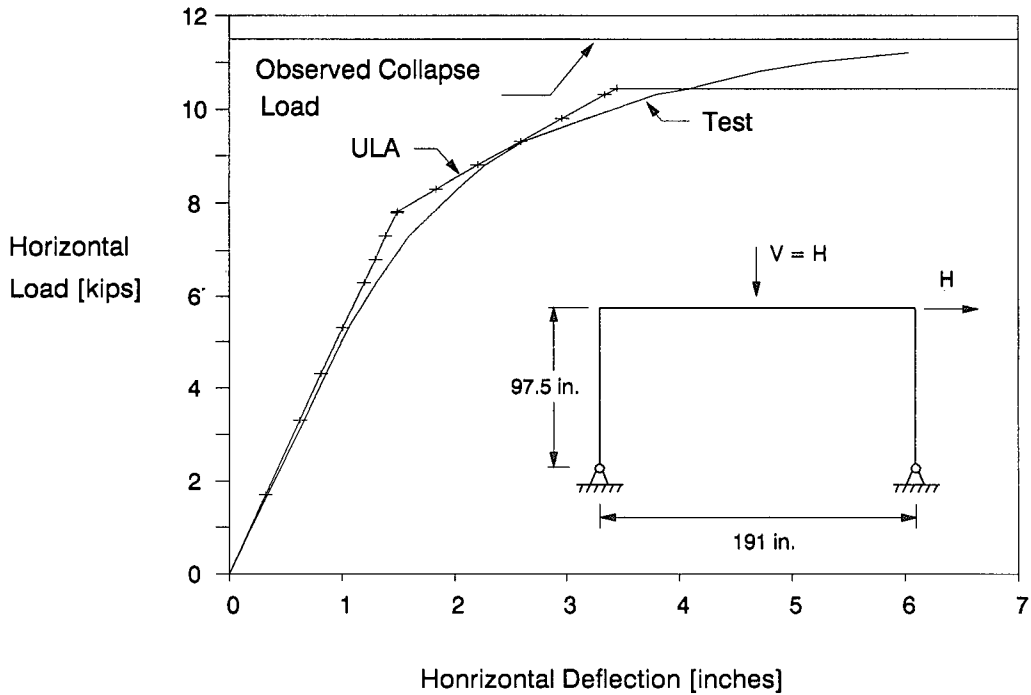


Figure 3.22: Load-Deflection Curves for Baker Test Frame

had to be approximated. The as-cut length of the column was given as $7' - 8\frac{1}{2}''$ (2350 mm), however, the distance from the base of the column to the center of the pin was not provided. From a photograph of the pin base, this dimension was approximated to be $5''$ (125 mm), thus giving the total column height of $8' - 1\frac{1}{2}''$ (2475 mm) used in ULA. Figure 3.22 shows that the results from ULA compare well in the elastic range, and thus it was felt that the above values were close to those existing in the test.

As can be seen in Fig. 3.22, the ultimate load from ULA is substantially lower, 10%, than the collapse load that was observed. However, this difference was believed to be the result of two factors. The first, and likely most important factor, is that the value of 33.8 ksi for σ_y is thought to be low. This is substantiated by the fact that Baker, using plastic collapse theory, predicted an ultimate load 3% lower than the measured value,

when it is well known that this theory provides an upper limit for the collapse load. The second factor is thought to be strain hardening, which was neglected by ULA. It was felt that the combination of these two factors caused the analytical collapse load to be lower than that of the test. However, the results from ULA are considered to be acceptable.

The examples shown here indicate that analytical results from ULA compare favourably with the test data. ULA very accurately modeled a simple column and also performed well with the two test frames. The 10% error seen in the examples is believed to be within acceptable design limits.

Chapter 4

Structures Within The Code Limits

4.1 Introduction

Within the applicability limits of the Canadian and American codes, there are an infinite number of possible structures. From these, four groups of single bay portal frames were chosen to give a wide range of design situations. These groups consist of fix-based frames to examine double curvature sway permitted columns, pin-based frames to examine single curvature sway permitted columns, laterally supported fix-based frames to examine double curvature sway prevented columns, and laterally supported pin-based frames to examine single curvature sway prevented columns. Within each group, stiff, intermediate and flexible frames were looked at, each of which carried a “large” and “small” percentage of the column axial capacity C_y , ($= 0.9A\sigma_y$) in the columns. The objective behind these selections was to check the codes against ULA for a wide range of loading conditions within the limitations set forth in the codes. The value for the yield stress used in ULA was $0.9\sigma_y$ such that the load at which the first hinge formed would be directly comparable to the Canadian code design, which uses $\phi = 0.9$.

4.2 Group One : Fix-Based Portal Frames

4.2.1 General

The fix-based portal frame shown in Fig. 4.23 was subjected to two constant vertical loads, each P, and a variable horizontal load, H. Three slenderness ratios were chosen for

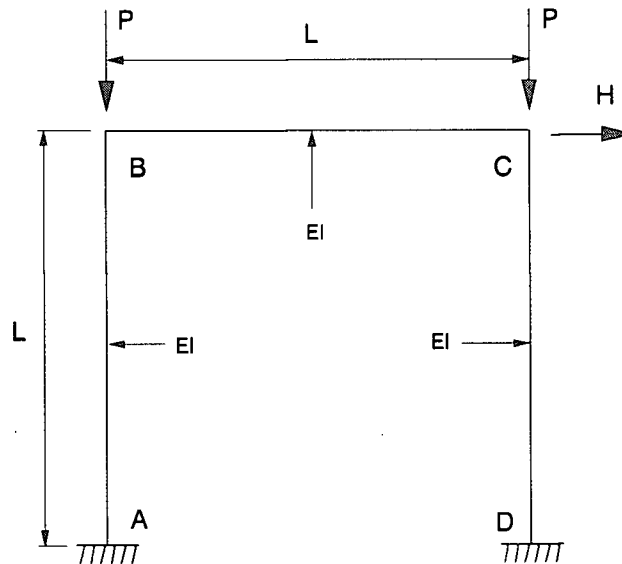


Figure 4.23: Fix-Based Portal Frame

the members of the frame, namely $L/r = 20, 100, 150$, to represent stiff, intermediate, and slender frames. At each slenderness ratio, two vertical load cases were analyzed: for $L/r = 20$, $P/C_y = 0.8$ and 0.2 ; for $L/r = 100$, $P/C_y = 0.4$ and 0.2 ; and for $L/r = 150$, $P/C_y = 0.2$ and 0.1 . For clarity purposes, the resulting six frames will be referred to as FIX20(0.8), FIX20(0.2), FIX100(0.4), FIX100(0.2), FIX150(0.2), and FIX150(0.1) respectively. The horizontal load in each frame was increased until the first hinge formed, which formed at D for all frames except FIX150(0.1) where it formed at A. The load was then increased until collapse, provided the frame did not fail after the first hinge, to show the amount of reserve capacity each frame had.

4.2.2 Canadian Code Design, Fix-Based Frames

Recall from Section 1.3 that the three design equations for beam columns are as follows:

$$\frac{M_f}{\phi Z \sigma_y} \leq 1.0 \quad (4.31)$$

$$\frac{C_f}{\phi A \sigma_y} + \frac{0.85 M_f}{\phi Z \sigma_y} \leq 1.0 \quad (4.32)$$

$$\frac{C_f}{C_r} + \frac{\omega M_f}{\phi Z \sigma_y \left(1 - \frac{C_f}{C_e}\right)} \leq 1.0 \quad (4.33)$$

The maximum horizontal load that the Canadian code allows each frame to carry was calculated using Eqs. 4.31 through 4.33. A value of 1.15 for k , obtained from the sway permitted nomograph, was used for the linear designs while a value of 0.63, obtained from the sway prevented nomograph, was used for the second order designs. The value of ω was 0.4 for the second order designs and 0.85 for the linear designs. It is interesting to note that for the linear designs, the stability equation, Eq. 4.33, governed the design of all six frames. However, for the second order design, the first strength equation, Eq. 4.31, governed the design of FIX150(0.1) and the second strength equation, Eq. 4.32, governed the design of the remaining five frames.

The results from the code equations have been non-dimensionalized and are shown with the results from ULA in Table 4.2. Note: a dash indicates that the code restricts the value of P to less than that applied, and thus the frame under the loads shown is not allowed.

4.2.3 American Code Design, Fix-Based Frames

Recall from Section 1.4 that the design equations are as follows:

$$\frac{C_f}{\phi_c C_n} + \frac{8M_f}{9\phi_b M_n} \leq 1.0 \quad \frac{C_f}{\phi_c C_n} \geq 0.2 \quad (4.34)$$

$$\frac{C_f}{2\phi_c C_n} + \frac{M_f}{\phi_b M_n} \leq 1.0 \quad \frac{C_f}{\phi_c C_n} < 0.2 \quad (4.35)$$

Frame	ULA				Canadian		American	
	Hinge #1	#2	#3	#4	Second Order	Linear	Second Order	Linear
FIX20(0.8)	0.633	0.702	0.743	0.753	0.633	0.513	0.367	0.367
FIX20(0.2)	2.644	2.907	3.122	3.206	2.644	2.611	2.477	2.477
FIX100(0.4)	0.468				0.468	—	—	—
FIX100(0.2)	1.859	1.875			1.859	0.910	0.990	1.005
FIX150(0.2)	0.295				0.295	—	—	—
FIX150(0.1)	1.835	1.844			1.835	0.956	0.870	0.783

Table 4.2: $\frac{HL}{0.9Z\sigma_y}$ Values For Fix-Based Frames

The values of k used in Eqs. 4.34 and 4.35 were the same as those used in the Canadian designs. The maximum horizontal load that the American code allows each frame to carry has been non-dimensionalized in Table 4.2. As with the Canadian code results, a dash indicates that the frame under the applied loads is not allowed.

Note from Table 4.2 that the American code is much more conservative than its Canadian counterpart for these frames. Also note that the difference between the linear and second-order designs is almost nonexistent for the American code, yet is quite substantial for the Canadian code. This is the result of the excellent approximation for M_{max} used in the linear formulation of the American design (Eq. 1.23) and the fact that, unlike the Canadian code, the value of C_n is the same for both the linear and second-order designs.

Due to the similarities in Eq. 4.33 of the Canadian code and Eqs. 4.34 and 4.35 of the American code, and the fact that the Canadian linear design is always governed by Eq. 4.33, the Canadian linear results are very similar to both the linear and second-order American results.

Also, because the Canadian failure surface, Eqs. 4.31 and 4.32, and a yield stress of $0.9\sigma_y$ were used in ULA, the load at which the first hinge formed and that given by the Canadian second-order design were identical.

4.3 Group Two : Pin-Based Portal Frames

4.3.1 General

The pin-based portal frame shown in Fig 4.24 was subjected to two constant vertical loads, each P , and a variable horizontal load, H . As was the case with the fix-based frame, three slenderness ratios were chosen for the members of the frame, namely $L/r = 20, 60, \text{ and } 100$. Two vertical load cases were analysed at $L/r = 20$ and 60 , while only one was analyzed at $L/r = 100$. These were $P/C_y = 0.8$ and 0.2 for $L/r = 20$, $P/C_y = 0.3$ and 0.2 for $L/r = 60$, and $P/C_y = 0.1$ for $L/r = 100$. Again, for clarity purposes, the five frames will be referred to as PIN20(0.8), PIN20(0.2), PIN60(0.3), PIN60(0.2), and PIN100(0.1) respectively. The horizontal load in each frame was increased until the first hinge formed, which formed at C in all frames except PIN100(0.1) where it formed at B. As with the fix-based frame, the load was then increased until collapse to show the amount of reserve capacity each frame had.

4.3.2 Canadian Code Design, Pin-Based Frames

The maximum horizontal load that the Canadian code allows each frame to carry was calculated using Eqs. 4.31 through 4.33. The value used for k was 2.29 (sway permitted nomograph) for the linear design and 0.88 (sway prevented nomograph) for the second-order design. The value of ω was 0.6 for the second-order design and 1.0 for the linear design. As with the fix-based frames, the stability equation, Eq. 4.33, governed the linear design of all five frames. The second-order design of PIN100(0.1) was governed by the first strength equation, Eq. 4.31, and the design of the remaining four frames was governed by the second strength equation, Eq. 4.32.

The code results have been non-dimensionalized and are shown with the results from ULA in Table 4.3. Again, a dash indicates that the frame under the applied loads is not

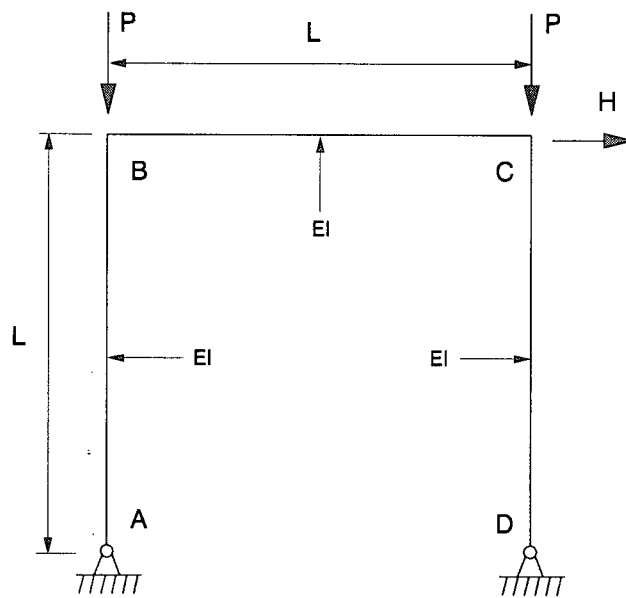


Figure 4.24: Pin-Based Portal Frame

Frame	ULA		Canadian		American	
	Hinge #1	#2	Second Order	Linear	Second Order	Linear
PIN20(0.8)	0.283	0.296	0.283	0.054	0.024	0.025
PIN20(0.2)	1.421	1.530	1.421	1.139	1.269	1.278
PIN60(0.3)	0.168		0.168	—	—	—
PIN60(0.2)	0.701		0.701	0.191	0.178	0.202
PIN100(0.1)	0.336		0.336	0.028	—	—

Table 4.3: $\frac{HL}{0.9Z\sigma_y}$ Values For Pin-Based Frames

allowed.

4.3.3 American Code Design, Pin-Based Frames

The maximum horizontal load that the American code allows each frame to carry was calculated using Eqs. 4.34 and 4.35. The values of k used in these equations were the same as those used in the Canadian design. The results have been non-dimensionalized and are shown in Table 4.2. As with the Canadian code results, a dash indicates that the frame is not allowed.

As with the previous example, notice that the Canadian linear and both American designs are very similar. Also, the Canadian second-order design and the first hinge given by ULA are the same. Both the Canadian linear design and the American designs are conservative with respect to ULA.

4.4 Group Three : Laterally Supported Fix-Based Portal Frames

4.4.1 General

The laterally supported fix-based portal frame shown in Fig 4.25 was subjected to two constant vertical loads, each P , and a variable distributed load, w . The three slenderness

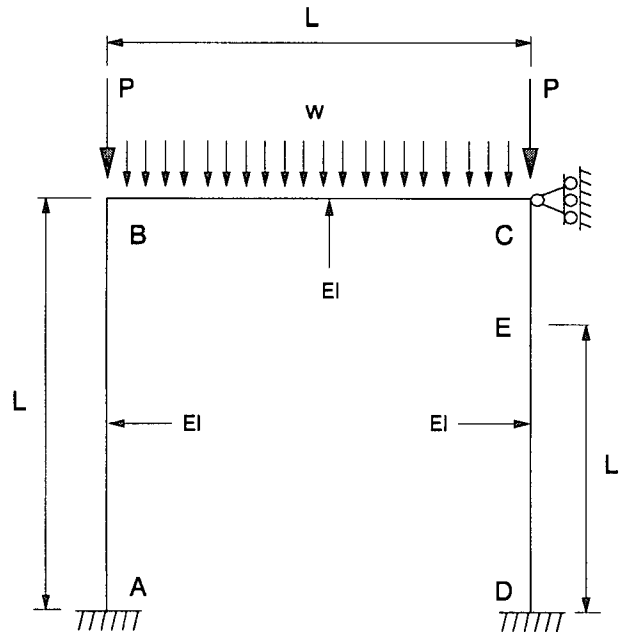


Figure 4.25: Laterally Supported Fix-Based Portal Frame

ratios chosen for the members of the frame were $L/r = 20, 60,$ and 100 . At $L/r = 20$ and 60 two vertical load cases were analyzed, while at $L/r = 100$ only one was analyzed. Namely, at $L/r = 20$, $P/C_y = 0.8$ and 0.2 , at $L/r = 60$, $P/C_y = 0.8$ and 0.4 , and at $L/r = 100$, $P/C_y = 0.4$. These five frames will be referred to as LSFIX20(0.8), LSFIX20(0.2), LSFIX60(0.8), LSFIX60(0.4), and LSFIX100(0.4) respectively. The “light” axial load of $P/C_y = 0.4$ for the intermediate and slender frames is higher than that used in the laterally unsupported examples, so as to ensure that the first hinge formed in the column rather than the beam.

The distributed load in each frame was increased until the first hinge formed, which in all cases formed at C. As with the unsupported frames, the load was then increased until collapse to show the amount of reserve capacity each frame had.

4.4.2 Canadian Code Design, Laterally Supported Fix-Based Frames

The maximum distributed load as allowed by the Canadian code for each frame to carry was calculated using Eqs. 4.31 through 4.33. The value used for k was 0.63 for both the linear and second-order designs. Also, the value of ω was 0.4 for the second-order design and 0.85 for the linear design. The linear design of all five frames was governed by the stability equation, Eq. 4.33. The second order design of LSFIX60(0.8) was governed by the stability equation, Eq. 4.33, while the design of the remaining five frames was governed by the second strength equation, Eq. 4.32. An extra joint was placed at L_1 ($0 < L_1 \leq L$) to determine whether the first hinge formed at the member end, C, or whether it formed somewhere within the member, at E. In all five cases, it was determined that the first hinge would form at C, i.e. the maximum moment in the column, M_{max} , occurred at the member end. Therefore, since M_f used in the design equations was already M_{max} (recall that M_f is the maximum end moment), it was believed that the strength equations would govern all five second-order designs. However, the stability equation governed the design of LSFIX60(0.8) as the value of C_r used in the equation built in enough conservatism to have it govern.

The results from the code equations are shown with the results from ULA in Table 4.4.

4.4.3 American Code Design, Laterally Supported Fix-Based Frames

The maximum distributed load that the American code allows each frame to carry was calculated using Eqs. 4.34 and 4.35. The values of k used in these equations were the same as those used in the Canadian design. The results have been non-dimensionalized and are shown in Table 4.4.

The American designs and the Canadian linear design show a slight deviation in this case, yet they are still comparable. Again, the Canadian second-order results are the

Frame	ULA			Canadian		American	
	Hinge #1	#2	#3	Second Order	Linear	Second Order	Linear
LSFIX20(0.8)	2.535	2.554	6.840	2.535	2.463	1.744	1.744
LSFIX20(0.2)	10.13	10.21	11.40	10.13	10.09	9.508	9.474
LSFIX60(0.8)	3.412	3.415	8.263	2.474*	1.237	0.928	0.928
LSFIX60(0.4)	6.729	6.738	9.803	6.729	4.640	4.640	4.640
LSFIX100(0.4)	11.31	11.32	11.63	11.31	6.075	7.811	6.943

* design governed by eq. 4.33

Table 4.4: $\frac{wL^2}{0.9Z\sigma_y}$ Values For Laterally Supported Fix-Based Frames

same as the first hinge results from ULA with the exception of frame LSFIX60(0.8). The reason for this discrepancy is that the governing equation for the Canadian design was the stability equation, Eq. 4.33, rather than the strength equation, Eq. 4.32. Notice from Table 4.4 that the Canadian linear results are close to the results from ULA for the stiff frames, yet deviate from the ULA results for the more flexible frames. This is due to the fact that C_r is equal to the axial capacity, C_y , for stiff columns and much lower than C_y for flexible columns. Again the code results are conservative when compared to the results from ULA.

4.5 Group Four : Laterally Supported Pin-Based Portal Frames

4.5.1 General

The laterally supported pin-based portal frame shown in Fig 4.26 was subjected to two constant vertical loads, each P, and a variable distributed load, w. The three slenderness ratios chosen for the members of the frame were $L/r = 20, 60,$ and 100 . The vertical load cases for each slenderness ratio were $P/C_y = 0.8$ and 0.2 for $L/r = 20$, $P/C_y = 0.8$ and 0.4 for $L/r = 60$, and $P/C_y = 0.4$ for $L/r = 100$. These five frames will be referred

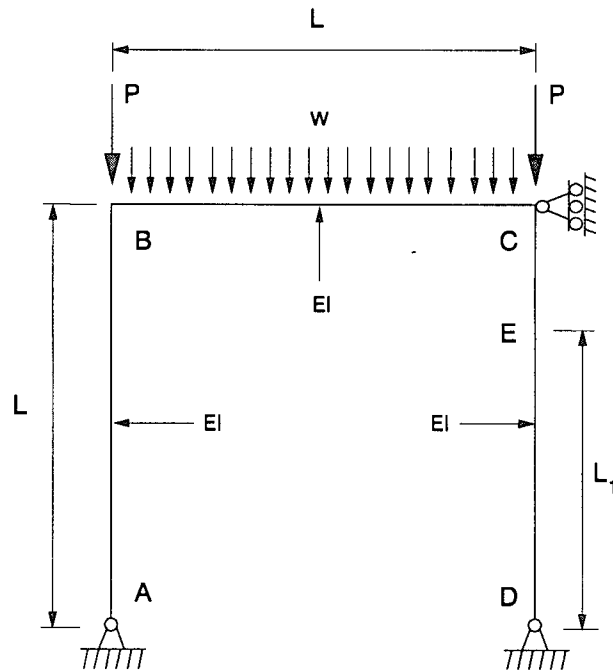


Figure 4.26: Laterally Supported Pin-Based Portal Frame

to as LSPIN20(0.8), LSPIN20(0.2), LSPIN60(0.8), LSPIN60(0.6), and LSPIN100(0.4) respectively.

The distributed load in each frame was increased until the first hinge formed, which in the case of LSPIN20(0.8) and LSPIN20(0.2) formed at C, and formed at E in the other three frames. As with the laterally supported fix-based frames, an extra joint was placed at E in order to locate where the first hinge formed.

Again, as with the unsupported frames, the load, w , was then increased until collapse to show the amount of reserve capacity each frame had.

4.5.2 Canadian Code Design, Laterally Supported Pin-Based Frames

The maximum distributed load that the Canadian code allows each frame to carry was calculated using Eqs. 4.31 through 4.33. The value used for k was 0.88 (sway prevented

nomograph) for both the linear and second-order designs. Also, the value of ω was 0.6 for the second-order design and 1.0 for the linear design. The linear design of all five frames was governed by the stability equation, Eq. 4.33. The second-order design of LSPIN20(0.8) and LSPIN20(0.2) was governed by the second strength equation, Eq. 4.32, while the design of the remaining three frames was governed by the stability equation, Eq. 4.33. The fact that the stability equation governed the design of these three frames is reassuring in this case, as the first hinge did not form at the member end. This indicates that the approximation for the maximum moment, $\omega M_f / \left(1 - \frac{C_f}{C_e}\right)$, is a good one. The results shown in Table 4.5 for these three designs are conservative when compared to ULA though, as the stability equation uses C_r rather than C_y as ULA does.

The results from the code equations are shown with the results from ULA in Table 4.5. A dash indicates that the frame under the applied axial load is not allowed by the code.

4.5.3 American Code Design, Laterally Supported Pin-Based Frames

The maximum distributed load that the American code allows each frame to carry was calculated using Eqs. 4.34 and 4.35. The values of k used in these equations were the same as those used in the Canadian design. The results have been non-dimensionalized and are shown in Table 4.5. A dash indicates that the frame is not allowed.

Note from Table 4.5 that unlike the previous examples, the American designs are quite different than the Canadian linear designs. Also, the Canadian second-order are only comparable to the results from ULA for the stiff frames. As was the case with the previous example, this was caused by the stability equation governing the design of the more flexible frames. As with the previous examples, the code results are conservative when compared to the results from ULA.

The Canadian and American codes are conservative for the four groups of frames illustrated here. However, the amount by which the codes are conservative varies greatly

Frame	ULA			Canadian		American	
	Hinge #1	#2	#3	Second Order	Linear	Second Order	Linear
LSPIN20(0.8)	2.736	2.744	6.840	2.736	2.155	1.744	1.744
LSPIN20(0.2)	10.91	10.94	11.41	10.91	9.542	10.16	10.12
LSPIN60(0.8)	3.649 ⁺	3.650		0.000*	0.000	—	—
LSPIN60(0.6)	7.598 ⁺	7.601		4.640*	2.784	4.022	3.712
LSPIN100(0.4)	9.196 ⁺			4.339*	1.736	6.075	4.339

⁺ hinge formed at E

* design governed by eq. 4.33

Table 4.5: $\frac{wL^2}{0.9Z\sigma_y}$ Values For Laterally Supported Pin-Based Frames

between frames. That is, the designer is unable to know whether the Canadian linear design, for instance, will result in a load that is ten or ninety percent of the load required to form the first hinge. Further, he is unable to know whether the American linear design will be more conservative than the American second order design or the Canadian linear design. It is the Authos opinion that this leaves the designer no room to use his judgement, and thus all he can do is follow the code and hope his design is adequate.

Chapter 5

Structures Beyond the Code Limits

5.1 Introduction

As was shown in the previous chapter, the code designs were adequate though conservative, for the chosen frames, Figs. 4.23 through 4.26. It is the purpose of this chapter to show where and why the codes may fail for more general structures. This will be accomplished through the use of several examples, each illustrating a different problem or reason for the codes failure. These structures will also be checked by the code equations and the results compared with those given by ULA. Because these structures are not within the code application limits outlined in Sec. 1.3.5, “reasonable” engineering assumptions were employed such that the code equations could be used. Although using the codes to design structures beyond the application limits of the codes is not a recommended practice, it is one that is often used by practicing engineers, and thus will be explored here.

5.2 Example Number One : Pin-Ended A-Frame

5.2.1 General

Contrary to what the building codes imply through the use of the sway prevented and sway permitted nomographs, the effective length of a column in a given structure is dependent on both the loading conditions and the structure itself. According to the nomographs, a column’s effective length depends only on its end conditions, or more

specifically, only the structure itself. The codes omit the loading dependency as they assume that all columns in the structure reach their critical load at the same time. If the structure were required to carry only one load combination, for example constant vertical loads only, an efficient design would have all of the columns in the structure reach their critical load at the same time. However, for more than one load combination, for example wind from both the left and right, this is no longer the case. Most structures are designed for different load combinations, thus one column in the structure will be “helped” by its neighbour and in the process its effective length will decrease below that given by the nomograph. Also in this process, the effective length of the neighbour will be increased. Clearly, the amount of support offered to the column depends on the axial load in the neighbour. If the neighbour has reached its critical load, no additional support will be afforded to the column in question. If, however, the neighbour is in tension, a large amount of support may be offered. This type of support will be referred to as “tension stiffening” in this paper. A structure that illustrates tension stiffening is the A-frame shown in fig. 5.27.

5.2.2 Effective Length Factor, k

The effective length of member CE in Fig. 5.27 depends on the angle of loading, θ . When the applied load is vertical, $\theta = 0^\circ$, both members AC and CE carry the same compression load. The result is that no support is given to member CE by member AC and the cross brace does nothing more than ensure that both members buckle in the same direction. That is, the effective length factor, k , of member CE under this loading is 1. When the load is horizontal, $\theta = 90^\circ$, member AC is in tension while member CE is in compression. Thus, the cross brace effectively holds the center of member CE in line with its ends and the member buckles into the second mode shape and $k = 0.5$.

The effective length factor, k , of member CE was calculated for various loading angles,

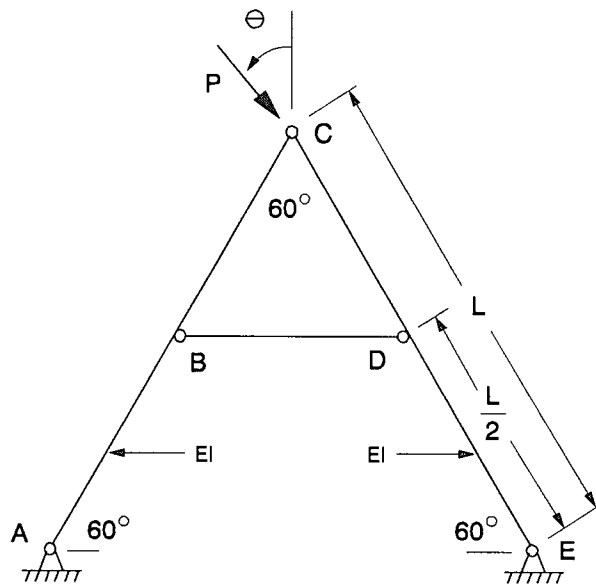


Figure 5.27: Pin-Ended A-Frame

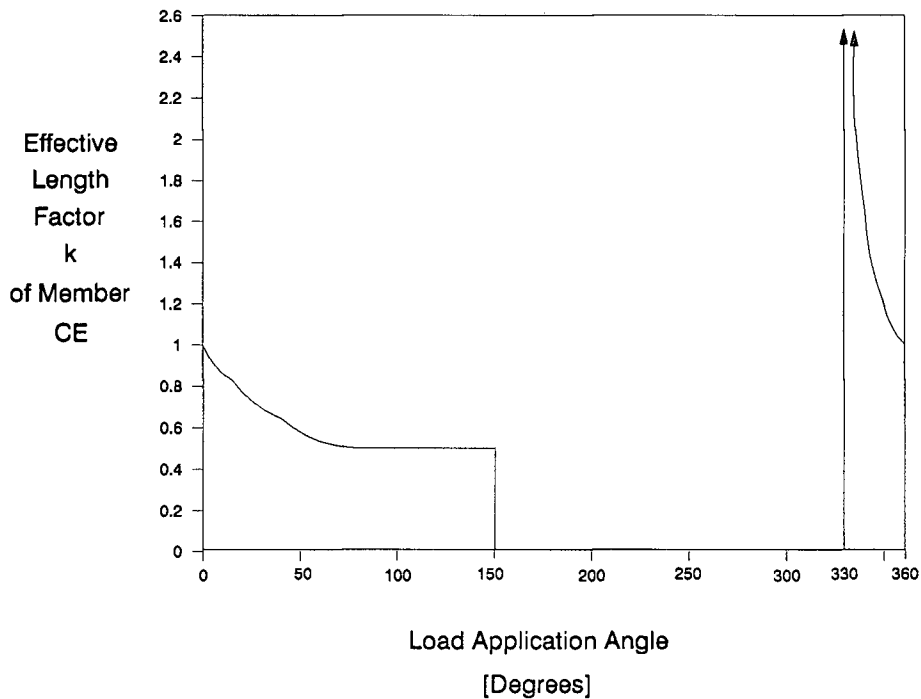


Figure 5.28: Variation of k Against θ for Member CE

$0^\circ < \theta \leq 360^\circ$, and the results are shown in Fig. 5.28. From the figure it can be seen that k is highly dependent on the loading conditions.

5.2.3 Code Design of Member CE

Vertical Load, No Tension Stiffening

The A-frame in Fig. 5.27 with $\theta = 0^\circ$ was modelled for ULA as shown in Fig. 5.29. The value $L/1000$ shown in the figure was chosen to represent the maximum fabrication eccentricity of a member. Also, the initial configuration of the member eccentricities was chosen to approximate the elastic buckled shape and thus result in the maximum moment occurring at D.

For the Canadian code design of member CE, recall from Sec. 1.3.1 that the three

design equations are:

$$\frac{M_f}{\phi Z \sigma_y} \leq 1.0 \quad (5.36)$$

$$\frac{C_f}{\phi A \sigma_y} + \frac{0.85 M_f}{\phi Z \sigma_y} \leq 1.0 \quad (5.37)$$

$$\frac{C_f}{C_r} + \frac{\omega M_f}{\phi Z \sigma_y \left(1 - \frac{C_f}{C_e}\right)} \leq 1.0 \quad (5.38)$$

It is important to realize that M_f is the maximum end moment. In the case of the A-frame, however, the end moments are zero. The commentary to the code does suggest using the midspan moment for a pin-ended column with a lateral distributed load, along with $\omega = 1$, for the linear design. There is no suggestions made for the second-order design though. The code also suggests that k for truss members can be assumed to be one, unless it can be shown that a smaller value is applicable. Therefore, it is proposed that M_f be replaced by the midspan moment, $C_f L/1000$, ω be one, and k also be one for the linear design. For the second-order design, it is proposed that the second-order moment at D be used in place of $\omega M_f / \left(1 - \frac{C_f}{C_e}\right)$ in Eq. 5.38. The reason for this is that $\omega M_f / \left(1 - \frac{C_f}{C_e}\right)$ is an approximation for the maximum moment in the member, and the second order midspan moment is the maximum moment. It is also proposed that the moment at D be used in place of M_f in Eqs. 5.36 and 5.37. Due to the C_f/C_r term in the stability equation and the assumptions above, Eq. 5.38 always governed the second order design. This does seem reasonable though, as the stability equation is in place to account for beam columns that have the hinge form within the member.

For the American code design of member CE, recall from Sec. 1.4 that the two design equations are:

$$\frac{C_f}{\phi_c C_n} + \frac{8M_f}{9\phi_b M_n} \leq 1.0 \quad \frac{C_f}{\phi_c C_n} \geq 0.2 \quad (5.39)$$

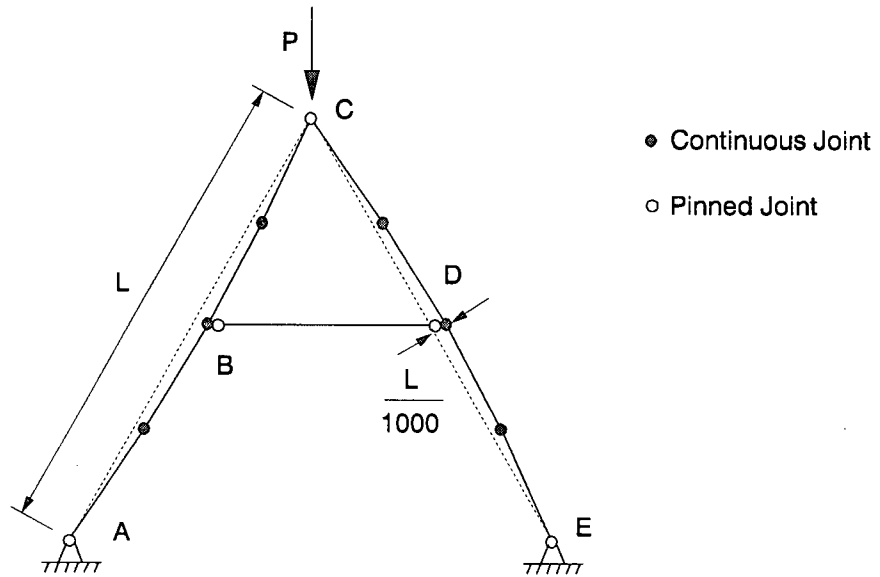


Figure 5.29: A-Frame Computer Model : Vertical Load

$$\frac{C_f}{2\phi_c C_n} + \frac{M_f}{\phi_b M_n} \leq 1.0 \quad \frac{C_f}{\phi_c C_n} < 0.2 \quad (5.40)$$

where:

$$M_f = B_1 M_{nt} + B_2 M_{lt} \quad (5.41)$$

For the same reasons set out in the Canadian design, it is proposed that the midspan moment be used in place of M_{nt} of Eq. 5.41 for calculation of M_f used in Eqs. 5.39 and 5.40. It is also proposed that $k = 1$ be used in calculating B_1 of Eq. 5.41. For the second-order design, the code suggests that M_f be the maximum member moment and thus the midspan moment was used.

The maximum axial load, C_f , that the codes allow member CE to carry using the above assumptions is shown in Table 5.6. This load has been non-dimensionalized and

Frame	ULA	Canadian		American	
		Second Order	Linear	Second Order	Linear
Fig. 5.29 $k = 1, \omega = 1$	0.585	0.387	0.390	0.416	0.419

Table 5.6: $\frac{P}{0.9A\sigma_y}$ Results For A-Frame : Vertical Load

is shown as a portion of the member's factored axial capacity, $0.9A\sigma_y$. The effect of this non-dimensionalizing procedure is that the results are independent of the 60° geometry angle shown in Fig. 5.27. The load given by ULA at which the first hinge formed has also been included in the table. It can be seen that the code equations give conservative results using the assumptions stated above when compared with the results of ULA, with the Canadian designs being more conservative than the American ones.

Horizontal Load, Includes Tension Stiffening

The A-frame in Fig. 5.27 with $\theta = 90^\circ$ was modelled for ULA as shown in Fig. 5.30. The value of $0.5L/1000$ was chosen to represent the maximum fabrication eccentricity of the member, in the shape shown in Fig. 5.30. Notice again that the initial configuration approximates the elastic buckled shape of the structure.

For the Canadian code design of member CE, the design equations are the same as those used for the vertical load case, Eqs. 5.36 through 5.38. The maximum moment for this case occurred at the quarter points, F and G. Thus for the same reasons as explained in the previous section, it is proposed that for the linear design, M_f be replaced by the linear moment at F, $C_f L/2000$, and that $\omega = 1$. For the second-order design, as with the vertical load case, it is proposed that the second-order moment at F replace $\omega M_f / \left(1 - \frac{C_f}{C_e}\right)$ in Eq. 5.38 and replace M_f in Eqs. 5.36 and 5.37.

Figure 5.28 shows that when $\theta = 90^\circ$, $k = 0.5$ for member CE. Thus, it is proposed

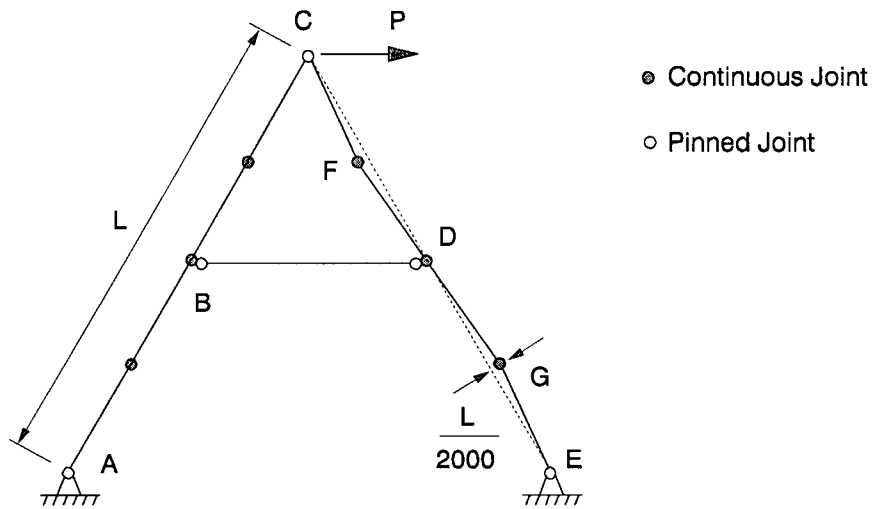


Figure 5.30: A-Frame Computer Model : Horizontal Load

Frame	ULA	Canadian		American	
		Second Order	Linear	Second Order	Linear
Fig. 5.29 $k = 1, \omega = 1$	0.992	0.424	0.426	0.461	0.461
Fig. 5.30 $k = 0.5, \omega = 1$	0.935	0.760	0.763	0.760	0.751

Table 5.7: $\frac{P}{0.9A\sigma_y}$ Results For A-Frame : Horizontal Load

that this value be used in the code equations. The code results using these assumptions are shown in Table 5.7. It is, however, possible that the designer would not realize that $k = 0.5$ for this loading condition. Thus, he might assume that $k = 1$ and use the configuration shown in Fig. 5.29. The results using these assumptions have therefore also been included in Table 5.7. It is clear from the table that $k = 0.5$ is a more appropriate value to use as $k = 1$ results in a highly conservative design.

For the American design of member CE, the code equations are the same as for the vertical load case, Eqs. 5.39 and 5.40. As with the Canadian design, it is proposed that the moment at F replace M_{lt} in Eq. 5.41. It is also proposed that the configuration of Fig. 5.30 be used. As with the Canadian design, the engineer might use the configuration in Fig. 5.29, and thus the results using both cases have been included in Table 5.7.

Also included in the table are the results from ULA assuming both the configuration in Fig. 5.29 and Fig. 5.30. It is clear that the results from ULA are less sensitive to the assumed deflected configuration than the code equations are, though the results using the configuration in Fig 5.29 are slightly unconservative.

A definite advantage of a computer program such as ULA now becomes clear. The effective length of each member in a structure can be easily found by slowly increasing the load until the structure buckles elastically. This buckling load is independent of any initial eccentricities such as those used in Figs. 5.29 and 5.30. The buckled shape will

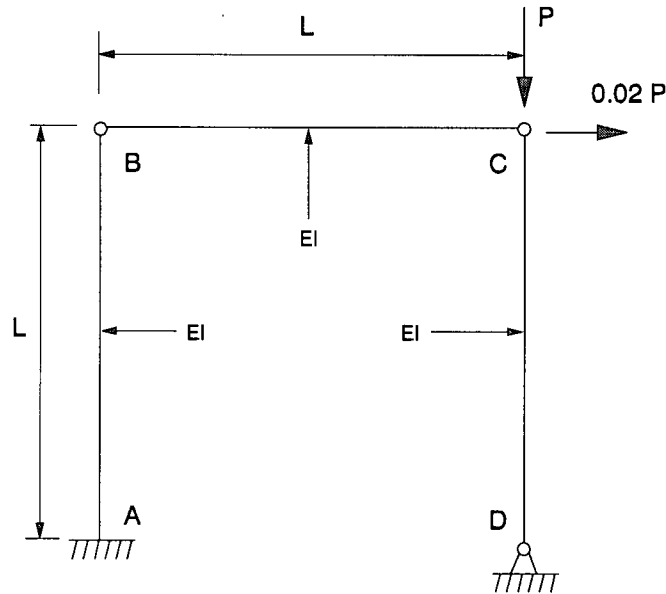


Figure 5.31: Single Fix-Based, Pin-Ended Frame

then shed light on what shape of eccentricities should be assumed, as if the eccentricity pattern follows the Eigenvector for the structure, the analysis will produce the largest moments of any such pattern.

5.3 Example Number Two : Single Fix-Based, Pin-Ended Frame

5.3.1 General

The frame shown in Fig. 5.31 is unusual in that the linear moment at A is amplified even though member AB carries no axial load. Since the frame is statically determinant, it is easy to show that the second-order moment at A is given by:

$$M_A = 0.02PL \left[\frac{1}{1 - \frac{PL^2}{3EI}} \right] \quad (5.42)$$

$$\text{or } M_A = \frac{M_L}{1 - \frac{P}{C'_e}} \quad (5.43)$$

where:

M_A = Second-order moment at A

M_L = Linear moment at A ($= 0.02PL$)

C'_e = Equivalent Euler load for AB ($= 3EI/L^2$)

Notice that the amplification factor in Eq. 5.43 is dependant on the entire structure rather than the member alone.

5.3.2 Code Design

Since the axial load, C_f , in member AB is zero, both the Canadian and American code equations reduce to the following:

$$\frac{M_f}{0.9Z\sigma_y} \leq 1.0 \quad (5.44)$$

The Canadian linear design takes no account of the moment amplification shown in Eq. 5.42 when calculating M_f in Eq. 5.44, and therefore it is unconservative. The American linear design, on the other hand, has taken this moment into account. Recall from Sec. 1.4 that M_f is as follows:

$$M_f = B_1M_{nt} + B_2M_{lt} \quad (5.45)$$

where in this case

$$B_1 = 0 \quad (5.46)$$

ULA	Canadian		American	
	Second Order	Linear	Second Order	Linear
0.452	0.452	1.000	0.452	0.452

Table 5.8: $\frac{0.02PL}{0.9Z\sigma_y}$ Values For Single Fix-Based, Pin-Ended Frame

and

$$B_2 = \frac{1}{1 - \sum C_f \left(\frac{\Delta_{ob}}{\sum H_f L} \right)} \quad (5.47)$$

It can be shown that the amplified linear moment given by Eq. 5.45 is the same as the second-order moment shown in Eq. 5.42.

Because a second order analysis automatically takes this type of amplification into account when calculating the moment, both the Canadian and American second-order designs agree with the results from ULA. These results are shown with the linear design results in Table 5.8. All of the results have been non-dimensionalized with respect to the factored plastic moment resistance, $0.9Z\sigma_y$. The American code is gives results which correlate with the results from ULA and which seem to be more exact for this type of frame than the Canadian code results.

The frame shown in Fig. 5.31 is simplistic yet it clearly shows that the classic amplification factor, $1 / \left(1 - \frac{C_f}{C_e} \right)$, does not always apply. As was the case in the previous example, this example further illustrates how one column “helps” its neighbour. More importantly for design purposes, however, this case shows how member CD is making member AB work harder than the Canadian linear design implies.

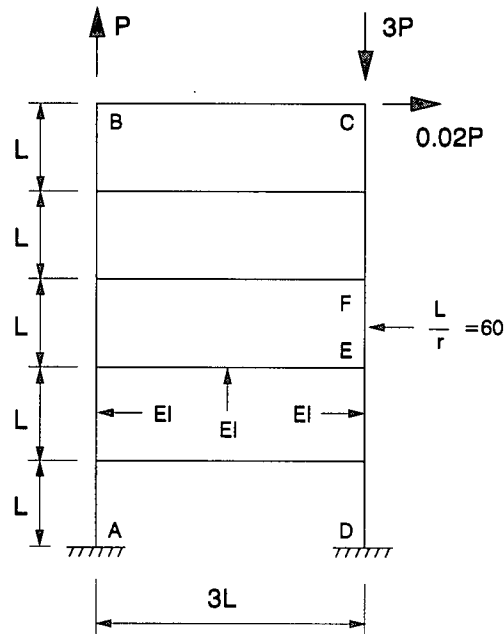


Figure 5.32: Five Storey Frame: Tension on One Side

5.4 Example Number Three : Five Storey Frame, Tension on One Side

5.4.1 General

The frame shown in Fig. 5.32 is intended to be a model of the first five storeys of a multi-storey frame subjected to a lateral wind load. Also, it could model a bent with some dead and out of plane torsional loadings. In either case the loading conditions are such that the columns in one side of the frame are in tension while the others are in compression. Note that the frame satisfies the code limitations, however the loading does not. That is, the loading is such that the columns in tension will help to stabilize the columns in compression.

ULA	Canadian		American	
	Second Order	Linear	Second Order	Linear
0.854	0.854	0.467	0.496	0.493

Table 5.9: $\frac{3P}{0.9A\sigma_y}$ Results For Five Storey Frame

5.4.2 Code Design

The code design results for member EF, the governing member, are shown in Table 5.9. The maximum load $3P$ that the codes allow the structure to carry has been non-dimensionalized with respect to the factored axial capacity, $0.9A\sigma_y$. Due to the symmetry of the structure, the moment used in the code equations was the usual maximum end moment and the effective length was calculated in the standard way using the nomographs. That is, no judgement was required when deciding what values of k and M_f to use.

When calculating the American linear results, the amplification factor B_2 in Eq. 5.47 includes the term $\sum C_f$, the sum of the axial loads in a storey. In this case, $\sum C_f = 3P-P$ and thus $2P$ was used in the formulation. The results shown in Table 5.9 show that this does in fact take account of the tension stiffening provided to member EF by the columns between A and B, as the linear and second-order American results are virtually identical.

Notice that the Canadian linear results are slightly lower than those of the American designs, while the Canadian second-order results are the same as those from ULA.

5.5 Example Number Four : Four Storey Frame, Multiple Column Lengths

5.5.1 General

The frame shown in Fig. 5.33 was chosen to show what effect different column lengths within a structure would have on the design of the members. Due to the one short storey,

ULA	Canadian		American	
	Second Order	Linear	Second Order	Linear
0.453	0.453	0.431	0.417	0.398

Table 5.10: $\frac{P}{0.9A\sigma_y}$ Results For Four Storey Frame

to the low L/r of member BD. However, after further investigation, it was discovered that there was a large discrepancy between the axial and moment contributions to the Canadian design equations. The linear design underestimated the moment contribution, $M_f/M_r \left(1 - \frac{C_f}{C_c}\right)$, when compared to the second order design. However, this underestimation was countered by an overestimation in the axial contribution, $C_f C_r$. To verify that this discrepancy was not only a function of the column slenderness chosen, the section used was changed such that L/r was 50 rather than 33. The result was that the linear and second-order designs became even closer to the results from ULA.

Two conclusions can be drawn from the previous results. First, the design equations were chosen to be conservative such that the design of structures of this type would be adequate. Second, the codes were fortunate in this case and a correct answer does not imply a correct solution. The Author favours the second of these conclusions.

5.6 Example Number Five : Tied and Fixed Arch

5.6.1 General

A common misconception among designers is that if one adds supports to a structure, it becomes stiffer or stronger. To illustrate that this is not the case, both arches shown in Fig. 5.34 were analysed with ULA. In both cases, the distributed load was increased until elastic buckling occurred, in order to find the effective length of a typical arch member

AB. As is illustrated by the buckled shapes shown in the figure, the effective length of AB is approximately $0.5L$ for Case 1, where both supports are fixed against translation, and approximately $0.09L$ for Case 2, where one support is released to translate freely. The reason for such a large difference in k is the tension stiffening provided to the arch by the tie when the support is released. When the support is restrained, Case 1, the tie carries only secondary forces and thus provides no support to the arch.

Unfortunately, the arches shown in Fig. 5.34 are so far removed from the code limitations (for example what is a girder and what is a column?) that it was felt that to compare code results with the results from ULA would be of little benefit. Thus the code designs for this example have been omitted. However, the example does illustrate the effect that tension stiffening can have on the overall behaviour of a structure.

5.7 Example Number Six : Overpass

5.7.1 General

As was shown in the previous example, it is often difficult for a designer to determine which members in a structure are acting as girders and which as columns when calculating the effective length factors for the code equations. Another common structure that illustrates this is the overpass shown in Fig. 5.35. It is a relatively simple task to design the legs, member BC and member DF, as they are simple compression members. However, the design of the girder is another matter. One design practice may be to assume the effective length of the center span, member CD, is $1.0L$. Another may be to ignore the axial load in the member completely. Both of these practices would be incorrect and un-conservative. ULA gives an effective length for the center span of the overpass as $1.36L$. Further, the axial load reduces the moment capacity by approximately twenty percent.

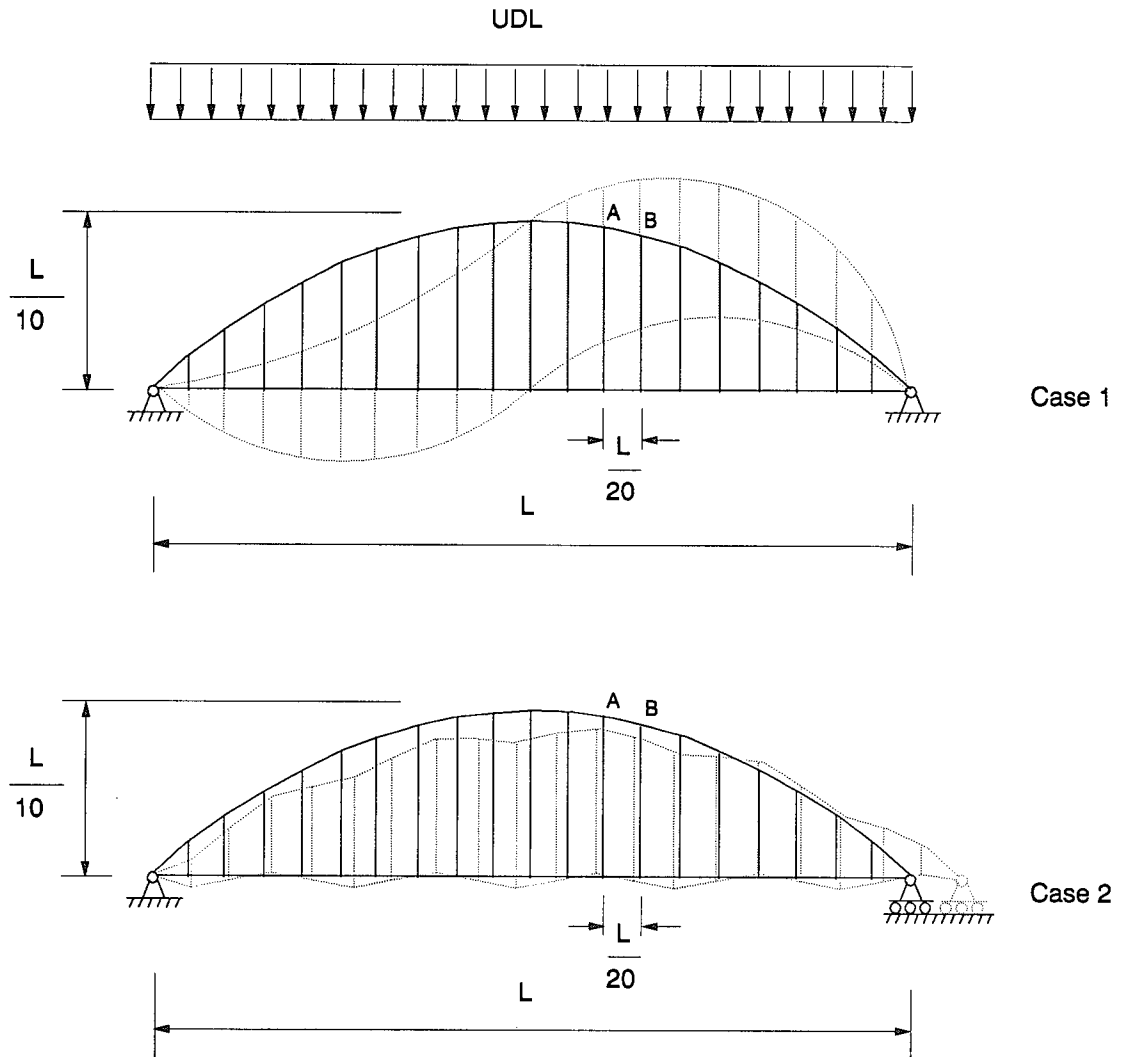


Figure 5.34: Fixed And Tied Arch

If the designer were to interpret the code in such a way that the parts of the deck carrying no axial load, member AC and member DE, were acting as girders and the center span, member CD, as a column, the side-sway permitted effective length factor would be 1.31. If one were to further assume that, because of the pin ended connection of the end spans, they provide three quarters of the rotational stiffness of fix ended members ($3EI/L$ rather than $4EI/L$), the effective length factor would be 1.43. These values appear to be reasonable when compared to the value given by ULA. However, with the previous examples in mind, one should be cautious when interpreting the code in this manner. Without the computer program to compare these values to, the designer could not be sure of the values given by his assumptions.

Due to the above arguments, as was the case with the previous example, it was felt that little insight would be gained through the comparison of the codes and ULA. Thus, the code results have been omitted.

The five examples illustrated here do not cover all possible design situations an engineer will face. However, they illustrate that for common structures, the building codes do not always work. The study presented here indicates that the codes are inconsistent, varying between being highly conservative and in one case highly unconservative. Thus the designer must be skeptical of the results given by the codes. Unfortunately, this is not always the case. Many designers feel that the codes are always conservative and thus a design by the code will work.

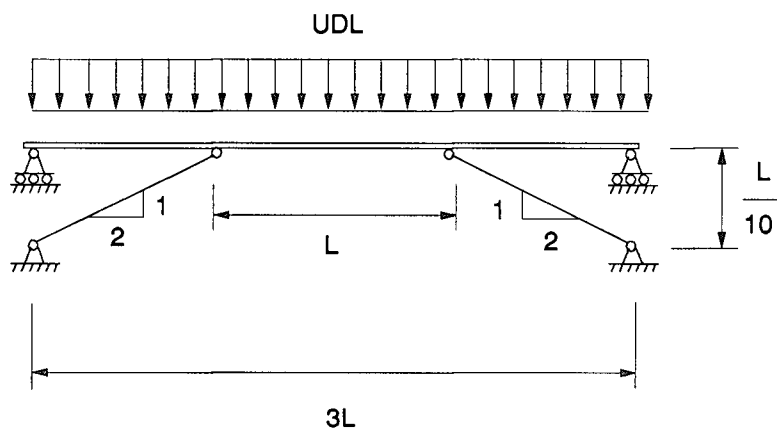


Figure 5.35: Overpass

Chapter 6

Conclusions And Recommendations

6.1 Conclusions

Because of their importance and wide spread use, the beam column design rules of both the Canadian and American building codes (CAN3-S16.3-M84 and LRFD 1986 respectively) were reviewed. It was noted that both codes offer the engineer two design options, the use of a linear analysis or the use of a second-order analysis.

An alternative design method was then proposed in the form of a second-order computer program, ULA. ULA was verified to within 10% by comparing other researchers test data to ULA's analytical results. In the case of a pin ended column, ULA gave results that compared well with the test results. ULA also compared well with two test frames, one by Yaramci and the other by Baker.

Accepting now that ULA gives an accurate representation of what actually happens in a loaded structure, the Canadian and American building code designs were compared to the analytical results of ULA for a wide range of structures. First the comparison was made for structures that satisfied the limitation requirements of the codes. It was found that the codes were conservative by as much as 90% when compared to the results from ULA for these structures, with the Canadian second-order designs being very similar to the results from ULA. Also, the Canadian linear results were similar to both the American linear and second-order designs for these structures.

Results from ULA were compared to the codes for structures beyond the code limits.

It was found for some cases that the codes gave results that were as conservative as 55%, for one case results that were 120% unconservative, and for others the results were very accurate when compared to results from ULA. Further, it was discovered that one could not reasonably predict whether the codes would be conservative or not. In all cases, the Canadian second-order design was closest to the results from ULA, and for the examples chosen, conservative.

With this in mind, the Author concludes that the use of a linear design procedure is not good enough anymore. The rapid advances made in computer technology in the recent past has made second-order design procedures both efficient and practical.

6.2 Recommendations

It is proposed that the code committees look into abolishing the use of linear design procedures in favour of more accurate second-order procedures. Further, the American code committee should reevaluate their decision to eliminate the strength equations such as those presented in CAN3-S16.3-M84. The adoption of these recommendations would need to be accompanied by changes in the load factors used in the codes. The current load factors, combined with the linear design procedures, presumably result in an adequate probability of failure among different structures. The more refined second-order procedures would require different load factors to achieve the same probability of failure. If one accepts the results from ULA as being accurate, the examples illustrated in this thesis indicate that this would result in a more uniform probability of failure among different structures than currently exists. With the exception of cases where the stability equation governed the design, the Canadian second order design procedure gave results consistent with the results from ULA. This was unlike the linear design procedure and both American procedures, all of which gave erratic results when compared to the results

from ULA. It is believed that adoption of the recommendations presented here would be beneficial to both the design profession and society as a whole.

6.3 Further Research

A second-order design procedure such as that proposed here should to be used in conjunction with a probability based algorithm to decide what values are appropriate for the load factors. Also, model and full-scale tests should be performed to verify the procedures accuracy. To reduce the cost of full-scale testing, buildings which are slated for demolition could become an inexpensive laboratory.

Bibliography

- [1] Canadian Institute of Steel Construction, *Handbook of Steel Construction, Fourth Edition, 1985.*
- [2] *American Institute of Steel Construction, Manual of Steel Construction, Load and Resistance Factored Design, 1986.*
- [3] “Commentary on Plastic Design in Steel”, *American Society of Civil Engineering: Manual of Engineering Practice No. 41, 1971.*
- [4] *Beaulieu, D., Picard, A., “A Reevaluation of the Canadian Provisions Pertaining to Steel Beam-Column Design and Frame Stability”, Canadian Journal of Civil Engineers, Oct. 1987, pp.593-601.*
- [5] Massonnet, C., “Stability Considerations in the Design of Steel Columns”, *Proceedings of the American Society of Civil Engineers, Sept. 1959, pp.75-111.*
- [6] *Chen, W.F., Lui, E.M., Structural Stability : Theory and Implementation, 1987.*
- [7] Austin, W.J., “Strength and Design of Metal Beam-Columns”, *Proceedings of the American Society of Civil Engineers, April 1961, pp.1-32.*
- [8] *American Institute of Steel Construction, Manual of Steel Construction, 1963.*
- [9] Hooley, R.F., Mulcahy, F.X., “Nonlinear Analysis by Interactive Graphics”, *Canadian Society of Civil Engineers Annual Conference, 1982.*
- [10] *Gere, J.M., Weaver, W., Analysis of Framed Structures., Van Nostrand Reinhold Co., New York, 1965.*

- [11] Galambos, T.V., Ketter, R.L., "Columns Under Combined Bending and Thrust", *Proceedings of the American Society of Civil Engineers, April 1959, pp.1-30.*
- [12] Guide to Design of Metal Compression Members, Column Research Council, 1960.
- [13] Yaramci, E., "Incremental Inelastic Analysis of Framed Structures", *Ph.D. Thesis, Lehigh University, 1966.*
- [14] Baker, J.F., Roderick, J.W., "Tests on Full-Scale Portal Frames", Institution of Civil Engineers, Paper No. 5838, 1952, pp.71-94.
- [15] *British Standards, BS4, Structural Steel Sections, 4:Part1, 1962.*